

Multiple imputation in functional regression with applications to EEG data in a depression study

Adam Ciarleglio^a, Eva Petkova^{b,c}, Ofer Harel^d

^a Department of Biostatistics and Bioinformatics, Milken Institute School of
Public Health, George Washington University, Washington, DC

^b Department of Population Health, New York University, New York, NY

^c Department of Child and Adolescent Psychiatry, New York University,
New York, NY

^d Department of Statistics, University of Connecticut, Storrs, CT

Abstract

Methods for estimating parameters in functional regression models require complete data on both the response and the predictors. However, in many applications, complete data are not available for all subjects. While many methods are available to handle missingness in data sets with all scalar variables, no such methods exist for data sets that include functional variables. We propose an approach that is an extension of multiple imputation by chained equations (fregMICE). fregMICE handles both scalar and functional variables as predictors in the imputation models as well as scalar and functional outcomes that need to be imputed. We also propose an extension to Rubin's Rules that can be used to pool estimates from the multiply imputed data sets and conduct valid inference. Simulation results suggest that the proposed methods are

superior to both complete case analysis and mean imputation in the context of estimating parameters in functional regression models. We employ the proposed methods in fitting a functional regression model for the relationship between major depressive disorder and frontal asymmetry curves derived from electroencephalography.

Keywords: functional data analysis, functional regression, missing data, multiple imputation, electroencephalography, major depressive disorder

1 Introduction

Functional data analysis (FDA) (Ramsay and Silverman, 2005) has become an important tool for understanding a host of complex data types generated in medical (Ratcliffe *et al.*, 2002a,b; Buckner *et al.*, 2004; Harezlak *et al.*, 2008; R. T. Ogden, 2010; Erbas *et al.*, 2010; Sørensen *et al.*, 2013; Ciarleglio *et al.*, 2015), economic (J. O. Ramsay, 2002; Besse *et al.*, 2005; Jank and Shmueli, 2006; Bapna *et al.*, 2008), environmental (Ogden *et al.*, 2002; Henderson, 2006; Ikeda *et al.*, 2008; Gao and Niemeier, 2008), and other application areas (Hutchinson *et al.*, 2004; Stewart *et al.*, 2006; Torres *et al.*, 2011). In particular, regression methods for functional data (Faraway, 1997; Cardot *et al.*, 1999; Marx and Eilers, 1999; Guo, 2002; James, 2002; Yao *et al.*, 2005; Morris and Carroll, 2006; Reiss and Ogden, 2007; Crambes *et al.*, 2009; James *et al.*, 2009; Crainiceanu *et al.*, 2009; Reiss and Ogden, 2010; Goldsmith *et al.*, 2011; Zhao *et al.*, 2012; Gertheiss *et al.*, 2013; Maronna and Yohai, 2013; McLean *et al.*, 2014; Zhu *et al.*, 2014; Ivanescu *et al.*, 2015; Scheipl *et al.*, 2015) have been widely developed and applied due to their ability to reveal complex patterns of association that are not discoverable when functional data are reduced to sets of scalars. It is reasonable to assume that FDA methods will become increasingly important as both the collection and storage of large amounts of functional data become simpler and cheaper.

Though many useful and powerful functional regression methods have been developed, they all assume that the data to which they are being applied consist of complete obser-

vations (i.e., no missing outcomes or predictors). There has been limited work on how to handle incomplete data in functional regression. Though Febrero-Bande *et al.* (2019) have considered missing scalar outcomes in functional regression, to our knowledge, there has been no research on how to handle settings where an entire function (whether playing the role of outcome or predictor) is missing. This is an important problem to consider, as missing data are becoming an issue in many studies that collect functional data.

Our interest in this problem is motivated by an investigation of the use of electroencephalography (EEG) data to distinguish between healthy control (HC) subjects and subjects with major depressive disorder (MDD) in the EMBARC clinical trial (Trivedi *et al.*, 2016). The EMBARC trial was conducted to search for biomarkers of antidepressant treatment response but the rich data available from the study can be probed to address other research questions related to MDD. Like many psychiatric conditions, MDD is a disease for which no clear biological markers currently exist. The state-of-the-art for diagnosis of MDD typically relies on self-reported symptom check-lists like those available in the DSM-5 (American Psychiatric Association, 2013). It has been argued that a more objective approach is needed to diagnose MDD and that the identification of reliable and specific biomarkers of MDD will provide a better understanding of the disease, which in turn may lead to the development of improved treatment strategies. To this end, investigators have focused their attention on trying to use neuroimaging tools to extract information about brain structure and function that may be useful in understanding the disease.

EEG is a neuroimaging modality that is particularly attractive since it is relatively low-cost, can be administered in resource limited settings, and is non-invasive. EEG measures changes in voltage across the scalp assumed to be related to gross neuronal activity. In the EMBARC trial, measurements were taken from multiple electrodes placed at various locations on the scalp using a standard headcap. The time-series data collected at each electrode underwent a sequence of processing steps and were transformed to the frequency domain in order to obtain current source density (CSD) power curves. These curves provide

information on the intensity of different rhythms/frequencies of neuronal activity for the subject (Tenke *et al.*, 2011). Frequency values are often divided into bands accordingly: from about 4 to 8 Hz is the theta band, about 8 to 16 Hz is the alpha band, and about 16 to 32 Hz is the beta band. Values outside of these bands may be of interest, but presently we restrict our attention to theta, alpha, and beta rhythms. A full description of the collection and processing of these data can be found in Tenke *et al.* (2017).

There is a large literature on the relationship between various summary measures derived from resting state EEG and depression. However, taken collectively, the results are generally inconclusive. One measure that has been studied repeatedly in relation to MDD is frontal alpha asymmetry (F α A): the difference in alpha power (μV^2) between right and left electrodes that are symmetrically located on the frontal region of the scalp. van der Vinne *et al.* (2017) conducted a meta-analysis of the association between F α A, using the F3 and F4 electrodes (locations shown in Figure 1), and depression status (MDD vs. HCs). They argue that gender (as well as age) may modify the association between depression status and F α A but that many previous studies have failed to account for these effects. Another limitation of these previous analyses is that F α A was analyzed as a single scalar value equal to the difference between the average power in the alpha band from the F4 electrode and average power in the alpha band from the F3 electrode (divided by the sum of the values to normalize inter-individual differences). We argue that this approach potentially discards relevant information by aggregating the CSD power curve (a function) to a single scalar summary measure. Since the CSD power curves are functional data, observed in the frequency domain, it may be advantageous to assess the association between frontal asymmetry (FA) and depression status using a functional data analytic approach. Furthermore, the EMBARC data provide an opportunity to investigate the association between FA beyond the alpha frequency band. The right panels of Figure 1 show the FA curves over the theta, alpha, and beta frequency bands for MDD and HC subjects in the EMBARC study stratified by gender. The FA curves are computed as $\frac{F4(t)-F3(t)}{F4(t)+F3(t)}$ for $t \in [4, 31.75]$ Hz where $F4(t)$ and

$F3(t)$ are the CSD power values at frequency t for the F4 and F3 electrodes, respectively. FA values are available at 112 frequencies ranging from 4 to 31.75 Hz in 0.25 Hz increments. An analysis on the scalar summary $F\alpha A$ values similar to that in van der Vinne *et al.* (2017) is equivalent to comparing the group-mean values corresponding to the dashed black lines over the 8 to 16 Hz band. We propose to fit a functional regression model with the FA curve as the outcome and disease status as the primary predictor of interest. Our goal is to characterize the relationship between disease status and FA across the 4 to 32 Hz range, while accounting for gender, age, and other relevant factors.

Unfortunately, some of the EEG data collected in the EMBARC study were flagged during quality control assessment as being “Unacceptable” or “Marginal” and therefore should not be used in our analysis. Still others were all together missing. In fact, Figure 1 displays only those FA curves for subjects with “Acceptable” or “Good” quality control designations. In addition, some of the values for the covariates that we wish to associate with FA are missing for some subjects. Instead of throwing out observations from subjects with incomplete data and conducting a complete case analysis, we have developed a multiple imputation (MI) procedure (Rubin, 1987; Schafer, 1997) for imputing the missing scalar and functional data and propose an approach for pooling estimates derived from the multiply imputed data sets.

Methods for performing MI with scalar data have been widely developed and research on methods development remains active, particularly in employing machine learning methods for fitting the imputation models (Burgette and Reiter, 2010; Doove *et al.*, 2014; Xu *et al.*, 2016; Zhao and Long, 2016; Zahid and Heumann, 2018). Furthermore, there are many powerful and user-friendly software packages that perform MI when the data consist only of scalar quantities, including, but not limited to software developed for R (R Development Core Team, 2018) such as *mice* (Buuren and Groothuis-Oudshoorn, 2011) and *Amelia* (Honaker *et al.*, 2011) and procedures developed for SAS (SAS Institute Inc, 2011) such as *PROC MI* and *PROC MIANALYZE*. We believe that similar methods and software should be available for handling functional data. To our knowledge, principled approaches for MI of functional

data have not been investigated in the literature nor has software been developed to perform MI with functional data. Here we propose an approach for performing MI with functional data and provide software for implementing the method.

The rest of the paper is structured as follows. In Section 2 we provide a brief overview of our target analysis models: functional regression models with either functional or scalar outcomes. In Section 3 we extend the missing data framework to include both scalar and functional data. In Section 4 we present a method for performing MI via chained equations with scalar and functional data. Section 5 presents the results of a simulation study, showing the validity and performance of the proposed imputation and pooling procedures. Section 6 illustrates the proposed method using data from the EMBARC trial. We conclude in Section 7 with a discussion and comments on possible directions of future research.

2 Review of Functional Regression Models

Functional regression refers to a broad category of models. If the response is a function and the predictors are functions, scalars, or both, then we refer to these as functional response models (FRMs). If the response is a scalar and the predictors are functions or both functions and scalars, then we refer to these as scalar response models (SRMs). Here, we briefly outline broad classes of FRMs and SRMs and methods for fitting them.

2.1 Functional Response Models (FRMs)

Suppose we collect a sample of n independent observations from a population of interest. For each observation, we have a function designated as the response, denoted by Y_i , p scalar variables, denoted by the p -dimensional vector $\mathbf{z}_i = (z_{i,1}, \dots, z_{i,p})^\top$, and q functional variables, denoted by the q -element set of functions $\mathbf{X}_i = \{X_{i,1}, \dots, X_{i,q}\}$ for $i = 1, \dots, n$. Assume that Y_i is a one-dimensional functional random variable that is square integrable on a compact support $I_Y \subset \mathbb{R}$ (i.e., $\int_{I_Y} Y_i^2(t) dt < \infty$). Similarly, assume that $X_{i,1}, \dots, X_{i,q}$ are

one-dimensional functional random variables that are each square integrable on a compact support $I_j \subset \mathbb{R}$ (i.e., $\int_{I_j} X_{i,k}^2(t)dt < \infty, k = 1, \dots, q$). For clarity, we assume that the functional predictors are observed without error but this need not be the case.

We model the relationship between the functional response and predictors with:

$$Y_i(t) \sim EF(\mu_i(t), \eta_t), \text{ such that } g\{\mu_i(t)\} = \beta_0(t) + \sum_{j=1}^p z_{i,j} \beta_j(t) + \sum_{k=1}^q \int X_{i,k}(s) \rho_k(s, t) ds. \quad (1)$$

In (1), $EF(\mu_i(t), \eta_t)$ corresponds to an exponential family distribution with mean $\mu_i(t)$ and dispersion parameter η_t , $g(\cdot)$ is a link function, $\beta_0(t)$ is the intercept function, $\beta_j(t)$ for $j = 1, \dots, p$ are the coefficient functions corresponding to the functional effects of the scalar predictors on the functional response, and $\rho_k(s, t)$ for $k = 1, \dots, q$ are the functional effects of the functional predictors on the functional response. This model can be simplified if additional information about the coefficient functions is known *a priori*. For example, if the effects of the scalar predictors are known to be constant over the domain of Y_i then we can model $\beta_j(t)$ as a constant for each j .

With complete data, we propose to estimate the coefficients in (1) using penalized function-on-function regression (PFFR) (Ivanescu *et al.*, 2015). Despite its name, the procedure allows for both scalar and functional predictors. PFFR can be implemented using well-documented software in the *refund* package (Goldsmith *et al.*, 2018) in R.

Briefly, the PFFR fitting procedure is carried out as follows. First, each coefficient function is represented by an appropriately selected set of basis functions (e.g., B-splines, cubic-regression splines, thin-plate splines, etc.). That is, we let $\beta_j(t) = \mathbf{B}_j^\top(t) \mathbf{b}_j$ for $j = 0, \dots, p$, where $\mathbf{B}_j(t) = (B_{j,1}(t), \dots, B_{j,L_j}(t))^\top$ is the vector of known basis functions selected for $\beta_j(t)$ and $\mathbf{b}_j = (b_{j,1}, \dots, b_{j,L_j})^\top$ is the corresponding vector of unknown basis coefficients. Similarly, we let $\rho_k(s, t) = \mathbf{U}_k^\top(s, t) \mathbf{u}_k$ for $k = 1, \dots, q$ where $\mathbf{U}_k(s, t) = (U_{k,1}(s, t), \dots, U_{k,L_k}(s, t))^\top$ is the vector of known bivariate basis functions (e.g., bivariate thin-plate splines) selected for $\rho_k(s, t)$ and $\mathbf{u}_k = (u_{k,1}, \dots, u_{k,L_k})^\top$ is the corresponding vector of unknown basis coefficients.

cients. The numbers of basis functions used in the representations (L_j and L_k) are typically selected to be larger than is assumed necessary to adequately represent a given function. The integral terms are approximated as $\int X_{i,k}(s)\rho_k(s,t)ds \approx \sum_{d=1}^{D_k} \Delta_d \rho(s_d, t) X_{i,k}(s_d) = \{\sum_{d=1}^{D_k} \mathbf{U}_k^\top(s_d, t) X_{i,k}(s_d) \Delta_d\} \mathbf{u}_k$, where s_d are the grid points over which $X_{i,k}$ is observed and Δ_d is the corresponding interval length between grid points. Substituting the integral approximation and basis representations into model (1) gives $g\{\mu_i(t)\} = \mathbf{B}_0^\top(t) \mathbf{b}_0 + \sum_{j=1}^p z_{i,j} \mathbf{B}_j^\top(t) \mathbf{b}_j + \sum_{k=1}^q \left\{ \sum_{d=1}^{D_k} \mathbf{U}_k^\top(s_d, t) X_{i,k}(s_d) \Delta_d \right\} \mathbf{u}_k$ and the log-likelihood function is given by $l(\mathbf{b}_0, \dots, \mathbf{b}_p, \mathbf{u}_1, \dots, \mathbf{u}_q) = \sum_{g=1}^{N_t} \sum_{i=1}^n \log [EF\{\mu_i(t_g | \mathbf{b}_0, \dots, \mathbf{b}_p, \mathbf{u}_1, \dots, \mathbf{u}_q), \eta_t\}]$, where $\{t_g; g = 1, \dots, N_t\}$ are the grid points at which Y_i is observed and we explicitly write the mean as a function of the vectors of parameters \mathbf{b}_j and \mathbf{u}_k for $j = 0, \dots, p$ and $k = 1, \dots, q$. As L_j and L_k are chosen to be large, smoothness in the estimated coefficient functions is achieved by including penalties on the estimated basis coefficients when maximizing the log-likelihood. Hence the objective function to be maximized is $l(\mathbf{b}_0, \dots, \mathbf{b}_p, \mathbf{u}_1, \dots, \mathbf{u}_q) - \sum_{j=0}^p \lambda_{\mathbf{b}_j} P_{\mathbf{b}_j}(\mathbf{b}_j) - \sum_{k=1}^q \lambda_{\mathbf{u}_k} P_{\mathbf{u}_k}(\mathbf{u}_k)$, where $P_{\mathbf{b}_j}(\mathbf{b}_j)$ and $P_{\mathbf{u}_k}(\mathbf{u}_k)$ are known penalty functions and $\lambda_{\mathbf{b}_j}$ and $\lambda_{\mathbf{u}_k}$ are the respective non-negative tuning parameters that control the amount of smoothness. Using quadratic penalties of the form $P_{\mathbf{b}_j}(\mathbf{b}_j) = \mathbf{b}_j^\top \mathbf{D}_{\mathbf{b}_j} \mathbf{b}_j$ and $P_{\mathbf{u}_k}(\mathbf{u}_k) = \mathbf{u}_k^\top \mathbf{D}_{\mathbf{u}_k} \mathbf{u}_k$, where $\mathbf{D}_{\mathbf{b}_j}$ and $\mathbf{D}_{\mathbf{u}_k}$ are known penalty matrices allows to use a mixed-effects model framework, with the coefficient functions viewed as random effects. In this setting, one can use restricted maximum likelihood (REML) to simultaneously select the tuning parameters and estimate the basis coefficients corresponding to the coefficient functions. Furthermore, approximate confidence intervals for the basis coefficients can be obtained. The estimated basis coefficients and their approximate intervals can then be substituted into the basis representations to obtain the estimated coefficient functions and point-wise confidence bands. Full details can be found in Ivanescu *et al.* (2015).

2.2 Scalar Response Models (SRMs)

Suppose that we observe \mathbf{z}_i and \mathbf{X}_i for $i = 1, \dots, n$ as above, but instead of having a functional response, we have a scalar response, y_i . We assume that the model of interest is the generalized functional linear model (McCullagh and Nelder, 1989; Cardot *et al.*, 1999):

$$y_i \sim EF(\mu_i, \eta), \text{ such that } g(\mu_i) = \theta_0 + \mathbf{z}_i \boldsymbol{\theta} + \sum_{j=1}^q \int X_{i,j}(t) \beta_j(t) dt. \quad (2)$$

In (2), $EF(\mu_i, \eta)$ corresponds to an exponential family distribution with mean μ_i and dispersion parameter η , $g(\cdot)$ is a link function, θ_0 is the intercept, $\boldsymbol{\theta}$ is a p -vector of scalar regression coefficients, and the coefficient functions $\beta_j(t)$ for $j = 1, \dots, q$ are square integrable on a compact support. The full collection of model parameters is denoted by $\boldsymbol{\nu} = \{\theta_0, \boldsymbol{\theta}, \beta_1, \dots, \beta_q\}$.

With complete data, we can use an appropriate method to obtain estimates for the scalar and functional coefficients, $\hat{\boldsymbol{\nu}} = \{\hat{\theta}_0, \hat{\boldsymbol{\theta}}, \hat{\beta}_1, \dots, \hat{\beta}_q\}$. Several methods exist for estimating parameters of SRMs. Here we consider penalized functional regression (PFR) (Goldsmith *et al.*, 2011) since it is able to handle both scalar and functional predictors as well as generalized scalar outcomes. PFR allows for sparse and/or error contaminated functional data as predictors, and a robust collection of computational tools exist for fitting and assessing these models in R (Goldsmith *et al.*, 2018).

Briefly, PFR is carried out as follows. First the functional covariates are represented using a truncated Karhunen-Loève decomposition, $X_{ij}(t) = \sum_{k=1}^{K_j} c_{ijk} \psi_{jk}(t) = \boldsymbol{\psi}_j(t) \mathbf{c}_{ij}$, where $\psi_{jk}(t)$ for $k = 1, \dots, K_j$ are the first K_j eigenfunctions (functional principal components (FPCs)) of the smoothed covariance operator corresponding to $cov\{X_{ij}(s), X_{ij}(t)\}$, $c_{ijk} = \int X_{ij}(t) \psi_{jk}(t) dt$ are the FPC scores, $\boldsymbol{\psi}_j(t) = (\psi_{j1}(t), \dots, \psi_{jK_j}(t))$ is a $1 \times K_j$ vector of the eigenfunctions, and $\mathbf{c}_{ij}^\top = (c_{ij1}, \dots, c_{ijK_j})$ is a $1 \times K_j$ vector of FPC scores representing the j -th functional covariate for the i -th subject. Next, each coefficient function, β_j , is represented using a suitable set of basis functions given by $\boldsymbol{\phi}_j(t) = (\phi_{j1}(t), \dots, \phi_{jL_j}(t))$ such that $\beta_j(t) = \sum_{\ell=1}^{L_j} b_{j\ell} \phi_{j\ell}(t) = \boldsymbol{\phi}_j(t) \mathbf{b}_j$, where $\mathbf{b}_j^\top = (b_{j1}, \dots, b_{jL_j})$. Using these representations, the right-

hand side of the equation in (2) can be re-expressed as $\theta_0 + \mathbf{z}_i\boldsymbol{\theta} + \sum_{j=1}^q \tilde{\mathbf{X}}_{ij}\mathbf{b}_j$ where $\tilde{\mathbf{X}}_{ij} = \mathbf{c}_{ij}^\top \mathbf{G}_j$ and \mathbf{G}_j is a $K_j \times L_j$ dimensional matrix with entry (u, v) given by $\int \psi_{ju}(t)\phi_{jv}(t)dt$.

As with the PFFR method to estimate the FRM given in (1), PFR uses a penalized log-likelihood objective function with similar penalties on the basis coefficients and employs a mixed effects model framework to obtain estimates for the basis coefficients. Using this framework, the basis coefficients are viewed as random effects in a mixed effects model and turning parameters are estimated via REML. As with PFFR, since PFR employs a mixed effects framework, it is possible to obtain approximate confidence intervals for the scalar coefficients and approximate point-wise confidence intervals for the coefficient functions. The reader is referred to Goldsmith *et al.* (2011) for the complete details of the PFR estimation procedure. K_j and L_j for $j = 1, \dots, q$ are tuning parameters that need to be chosen prior to estimation. Selection can be based on a data-driven approach such as cross-validation, but this approach may be computationally intensive. Alternatively, Goldsmith *et al.* (2011) note that as long as they are chosen “large enough,” then their specific values have minor impact on the quality of the estimates.

3 Missing Scalar and Functional Data

Formal treatment of missing data mechanisms and their corresponding models have been discussed extensively elsewhere (e.g., Rubin (1987); Little and Rubin (2002); van Buuren (2012)). Here we provide an overview of these concepts in settings with both scalar and functional data as well as an overview of MI.

3.1 Notation and Missingness Mechanisms

We start by relabeling the scalar and functional variables. If the response of interest is a scalar, then we let $y_i = w_{i,1}$, $z_{i,1} = w_{i,2}, \dots, z_{i,p} = w_{i,p+1}$, and $X_{i,1} = w_{i,p+2}, \dots, X_{i,q} = w_{i,p+q+1}$. If the response of interest is a function, then we let $z_{i,1} = w_{i,1}, \dots, z_{i,p} = w_{i,p}$,

$Y_i = w_{i,p+1}$, and $X_{i,1} = w_{i,p+2}, \dots, X_{i,q} = w_{i,p+q+1}$. Either way, the $p + q + 1$ variables can be gathered into an $n \times (p + q + 1)$ matrix of components, some of which are scalars and others are functions, $\mathbf{W} = (\mathbf{w}_1, \dots, \mathbf{w}_{p+q+1})$. $\mathbf{w}_i = (w_{i,1}, \dots, w_{i,p+q+1})^\top$ represents a random draw from a multivariate distribution having a set of unknown parameters denoted by $\boldsymbol{\xi}$. Let $\mathbf{R} = (\mathbf{r}_1, \dots, \mathbf{r}_{p+q+1})$ be an $n \times (p + q + 1)$ indicator matrix with entries $r_{i,j}$ such that $r_{i,j} = 1$ if $w_{i,j}$ is observed and $r_{i,j} = 0$ if $w_{i,j}$ is missing. Let \mathbf{W}^{obs} denote the observed components of \mathbf{W} and \mathbf{W}^{mis} denote the missing components of \mathbf{W} . The general expression for the missing data model is $P(\mathbf{R}|\mathbf{W}^{obs}, \mathbf{W}^{mis}, \boldsymbol{\psi})$, where $\boldsymbol{\psi}$ corresponds to the collection of parameters for the missing data model.

We extend the definitions used to classify missing data given in Little and Rubin (2002) to settings that include functional data. Data are missing completely at random (MCAR) if $P(\mathbf{R} = \mathbf{r}|\mathbf{W}^{obs}, \mathbf{W}^{mis}, \boldsymbol{\psi}) = P(\mathbf{R} = \mathbf{r}|\boldsymbol{\psi})$, that is, missingness only depends on the parameter(s) in $\boldsymbol{\psi}$, the overall probability of being missing. Data are said to be missing at random (MAR) if missingness depends on the observed information in the sample as well as the parameter(s) in $\boldsymbol{\psi}$, i.e., $P(\mathbf{R} = \mathbf{r}|\mathbf{W}^{obs}, \mathbf{W}^{mis}, \boldsymbol{\psi}) = P(\mathbf{R} = \mathbf{r}|\mathbf{W}^{obs}, \boldsymbol{\psi})$. Lastly, data are said to be missing not at random (MNAR) if missingness depends on both the observed and missing information in the sample as well as the parameter(s) in $\boldsymbol{\psi}$, i.e., $P(\mathbf{R} = \mathbf{r}|\mathbf{W}^{obs}, \mathbf{W}^{mis}, \boldsymbol{\psi})$ does not simplify.

Under MCAR and some MNAR settings (Bartlett *et al.*, 2014), a complete case analysis (CCA) yields unbiased estimates for the model parameters. However, these estimates may be inefficient in the sense that all data from the incomplete cases are being discarded. When there are many predictors, each prone to missing values, the size of the complete case data can be much smaller than the full set of observations. This can greatly limit one's ability to extract information from data with complex associations. When data are MAR, a CCA can lead to both inefficiency and bias in the parameter estimates for some settings. For example, in the regression setting, when missingness in the covariates depends on the value of the designated response, CCA yields biased estimates (White and Carlin, 2010). Under MAR

mechanism, missing data can be imputed using imputation models that provide predictions for the missing values. The assumption that data are MAR is not testable with available data but previous work suggests that the MAR assumption is approximately valid if the imputation model includes enough relevant variables (Schafer, 1997; Collins *et al.*, 2001; Harel and Zhou, 2007; White *et al.*, 2011; Harel *et al.*, 2014; Perkins *et al.*, 2018). In addition to the MAR assumption, we assume that the parameter spaces are distinct; $\boldsymbol{\psi}$ and $\boldsymbol{\xi}$ are distinct if the joint parameter space is equivalent to the product of the individual parameter spaces. The combination of MAR and parameter distinctness allows us to ignore the missingness indicators, \mathbf{R} , in likelihood or Bayes type inferences (Little and Rubin, 2002). This is considered as an ignorable model. In this paper, we focus on ignorable models settings, such that missing data that are MAR and $\boldsymbol{\psi}$ and $\boldsymbol{\xi}$ are distinct sets of parameters.

3.2 Joint and Imputation Models

Rubin (1987) provides a general framework to conduct imputation of missing data: imputation should follow from the specification of a joint model for $[\mathbf{W}, \mathbf{R}]$. Correct specification of such a model can be a complex task in settings with purely scalar data of mixed types (e.g., continuous, categorical, etc.) and is made even more complex in the present setting with functional data. Fortunately, we propose that high-quality imputations can be constructed without directly specifying this joint distribution. Instead, one can specify an imputation model, $f(\mathbf{W}^{mis} | \mathbf{W}^{obs}, \mathbf{R})$, which describes how missing values are generated. In MI, one draws from this distribution multiple times to create multiple complete data sets.

Conceptually, MI in settings with both scalar and functional data is similar to MI of purely scalar data with the goal being to use the distribution of the observed data to fill in plausible values for the missing data. As with purely scalar data, MI in the present setting can be justified using a Bayesian framework.

Under MAR and ignorability assumptions (and also under the stricter MCAR assump-

tion) the posterior predictive distribution for \mathbf{W}^{mis} is independent of \mathbf{R} and given by

$$f(\mathbf{W}^{mis}|\mathbf{W}^{obs}) = \int f(\mathbf{W}^{mis}|\mathbf{W}^{obs}, \boldsymbol{\xi})f(\boldsymbol{\xi}|\mathbf{W}^{obs})d\boldsymbol{\xi}, \quad (3)$$

where $f(\mathbf{W}^{mis}|\mathbf{W}^{obs}, \boldsymbol{\xi})$ is the predictive distribution of \mathbf{W}^{mis} given \mathbf{W}^{obs} and $\boldsymbol{\xi}$,

$$f(\boldsymbol{\xi}|\mathbf{W}^{obs}) \propto f(\boldsymbol{\xi}) \int f(\mathbf{W}^{mis}, \mathbf{W}^{obs}|\boldsymbol{\xi})d\mathbf{W}^{mis}, \quad (4)$$

is the observed-data posterior distribution for $\boldsymbol{\xi}$, and $f(\boldsymbol{\xi})$ is the prior distribution. Together, (3) and (4) point to a two-step method for MI: in the m -th imputation ($m = 1, \dots, M$), first make a random draw for $\boldsymbol{\xi}$ from its posterior distribution, denoted by $\hat{\boldsymbol{\xi}}^{(m)}$, then impute the missing values in \mathbf{W}_{mis} by a random draw from $f(\mathbf{W}^{mis}|\mathbf{W}^{obs}, \hat{\boldsymbol{\xi}}^{(m)})$ to obtain $\mathbf{W}^{mis(m)}$.

Meng (1994) showed that it is important that the imputation model be congenial with the analysis model (in our case this is either model (1) or (2)), otherwise the analysis of the imputed data can lead to inconsistent parameter estimates and/or biased estimates of variance. In practice the goal is to make it so that the imputation model is at least as general as the analysis model so as to avoid leaving out important predictors or associations that will be investigated in the analysis model. One way to make the imputation model more general is to include auxiliary variables that may be available, but that are not to be considered in the inference model. For simplicity, we do not consider auxiliary variables here, but will base the our imputation models only on those variables being considered in the inference model.

4 Multiple Imputation for Scalar and Functional Data

In the present setting, the imputation model may require the prediction of missing scalar values based on observed functional and/or scalar data as well as prediction of missing function values based on observed scalar and/or functional data. To predict missing scalar values, we propose to construct SRMs and use PFR. To predict missing function values, we

propose to construct FRMs and use PFFR. Below, we lay out the proposed imputation procedure. We do this first in the simplified case where only one variable has missing values and then extend the method to more general missing patterns. We end this section by showing how to combine results from the multiply imputed data sets.

4.1 Imputation Procedures

4.1.1 Simplified Case

For the sake of clarity, we begin by considering settings in which all but one variable, $\mathbf{w}_{\cdot j}$ (here the $\cdot j$ subscript emphasizes that this is column j of matrix \mathbf{W}), are completely observed. Without loss of generality, assume that the first r values in $\mathbf{w}_{\cdot j}$ are observed, denoted by $\mathbf{w}_{\cdot j}^{obs} = (w_{1,j}, \dots, w_{r,j})^\top$, and the last $n - r$ values in $\mathbf{w}_{\cdot j}$ are missing, denoted $\mathbf{w}_{\cdot j}^{mis} = (w_{r+1,j}, \dots, w_{n,j})^\top$. Define the complement data set to $\mathbf{w}_{\cdot j}$ by $\mathbf{W}_{-j} = (\mathbf{w}_{\cdot 1}, \dots, \mathbf{w}_{\cdot j-1}, \mathbf{w}_{\cdot j+1}, \dots, \mathbf{w}_{\cdot p+q+1}) = [\mathbf{W}_{-j}^{obs\top}, \mathbf{W}_{-j}^{mis\top}]^\top$.

The observed data are $\mathbf{W}^{obs} = \{\mathbf{w}_{\cdot j}^{obs}, \mathbf{W}_{-j}^{obs}, \mathbf{W}_{-j}^{mis}\}$ and the missing data are $\mathbf{W}^{mis} = \mathbf{w}_{\cdot j}^{mis}$ so that there are r complete observations and $n - r$ incomplete observations that are missing values for $\mathbf{w}_{\cdot j}$. In this setting, the imputation model in (3) can be expressed as

$$f(\mathbf{w}_{\cdot j}^{mis} | \mathbf{w}_{\cdot j}^{obs}, \mathbf{W}_{-j}) = \int f(\mathbf{w}_{\cdot j}^{mis} | \mathbf{W}_{-j}^{mis}, \boldsymbol{\xi}_j) f(\boldsymbol{\xi}_j | \mathbf{w}_{\cdot j}^{obs}, \mathbf{W}_{-j}^{obs}) d\boldsymbol{\xi}_j. \quad (5)$$

In order to obtain the posterior distribution $f(\boldsymbol{\xi}_j | \mathbf{w}_{\cdot j}^{obs}, \mathbf{W}_{-j}^{obs})$, we can specify and fit a regression model with $\mathbf{w}_{\cdot j}^{obs}$ as the response and \mathbf{W}_{-j}^{obs} as the predictors.

When $\mathbf{w}_{\cdot j}$ is one of the scalar variables (e.g., $w_{i,j} = z_{i,j}$ or y_i when the analysis model is

a SRM), we can employ a suitable SRM. For example, we use the model

$$z_{i,j} \sim EF(\mu_{i,j}, \eta_j) \text{ such that } h_j(\mu_{i,j}) = \gamma_{j,0} + \sum_{\ell \neq j} z_{i,\ell} \gamma_{j,\ell} + \alpha_j y_i + \sum_{k=1}^q \int X_{i,k}(t) \omega_{j,k}(t) dt,$$

or

$$h_j(\mu_{i,j}) = \gamma_{j,0} + \sum_{\ell \neq j} z_{i,\ell} \gamma_{j,\ell} + \int \alpha_j(t) Y_i(t) dt + \sum_{k=1}^q \int X_{i,k}(t) \omega_{j,k}(t) dt,$$

depending on whether the response Y for the analysis model is a scalar (top) or a function (bottom). The components of (6) are similar to those in analysis model (2) where the collection of parameters is $\boldsymbol{\xi}_j = \{\gamma_{j,0}, \gamma_{j,\ell(\ell \neq j)}, \alpha_j, \omega_{j,1}, \dots, \omega_{j,q}\}$, which can be estimated using PFR. When the error function corresponds to either the binomial or Poisson distribution, the i th subject's missing value for the j th variable can be filled in with a random draw from either distribution, using the predicted value of $\mu_{i,j}$. When the error function is normal, the i th subject's missing value for the j th variable can be filled in with the predicted value of $\mu_{i,j}$ with a random error term added to it. This random error term is drawn from the $N(0, \hat{\sigma}_j^2)$ distribution, where $\hat{\sigma}_j^2$ is estimated from the residuals under model (6).

When $\boldsymbol{w}_{\cdot j}$ is one of the functional variables (e.g., $w_{i,j} = X_{i,j}$ or Y_i when the analysis model is a FRM), we can employ a suitable FRM. For example, we use the model

$$X_{i,j}(t) \sim EF(\mu_{i,j}(t), \eta_{j,t}) \text{ such that } h_j\{\mu_{i,j}(t)\} = \gamma_{j,0}(t) + \sum_{\ell=1}^p z_{i,\ell} \gamma_{j,\ell}(t) + y_i \alpha_j(t) + \sum_{k \neq j} \int X_{i,k}(s) \omega_{j,k}(s, t) ds,$$

or

$$h_j\{\mu_{i,j}(t)\} = \gamma_{j,0}(t) + \sum_{\ell=1}^p z_{i,\ell} \gamma_{j,\ell}(t) + \int Y_i(s) \alpha_j(s, t) ds + \sum_{k \neq j} \int X_{i,k}(s) \omega_{j,k}(s, t) ds,$$

depending on whether the response Y for the analysis model is a scalar (top) or a function (bottom). The components of (7) are similar to those in analysis model (1) and the collection of parameters $\boldsymbol{\xi}_j = \{\gamma_{j,0}, \gamma_{j,1}, \dots, \gamma_{j,p}, \alpha_j, \omega_{j,k(k \neq j)}\}$ can be estimated using PFFR. The i th subject's missing value for the j th covariate can be filled in with the predicted value of

$\mu_{i,j}(t)$ with a random error function added to it. The random error function is generated as follows. First, we compute estimates of the leading principal component basis functions $\{\hat{\psi}_1, \dots, \hat{\psi}_K\}$ (accounting for at least 99% of the variance), the corresponding score variances, $\hat{\boldsymbol{\lambda}} = (\hat{\lambda}_1, \dots, \hat{\lambda}_K)^\top$, and mean function, $\hat{\mu}_r$, from a functional principal components decomposition of the collection of residual curves derived from fitting (7) on the observations for which the j th covariate is observed. Then we generate subject-specific principal component loadings, $\mathbf{c}_i = (c_{1,i}, \dots, c_{K,i})^\top$, from $\mathbf{c}_i \sim N(\mathbf{0}, \text{diag}(\hat{\boldsymbol{\lambda}}))$, and let $r_i(t) = \hat{\mu}_r(t) + \sum_{k=1}^K c_{ki} \hat{\psi}_k(t)$ be the random error function for the i th subject.

Both (6) and (7) can be fit using the `refund` package (Goldsmith *et al.*, 2018) in R. In order to account for uncertainty in the parameters involved in the imputation model, we propose to select a bootstrap sample from the complete data and obtain parameter estimates from fitting (6) or (7) on the bootstrap sample. The use of a bootstrap sample is suggested in van Buuren (2012) Section 3.1. The complete procedure is repeated M times to obtain M imputed data sets. Both (6) and (7) can be made more flexible by the addition of various interaction terms or by allowing for less restrictive functional forms for the coefficient functions. These modifications can also be handled using various functions from the `refund` package, but may increase the computational complexity of the imputation procedure.

4.1.2 General Missing Patterns and the fregMICE Algorithm

In the previous section we described how to impute data when only one variable is incomplete. When more than one variable are incomplete, we propose to employ multiple imputation by chained equations (MICE) (van Buuren and Oudshoorn, 1999) by extending the method to incorporate functional variables. MICE is conducted in a variable-by-variable manner via specification of a conditional model for each $\mathbf{w}_{\cdot j}$ ($j = 1, \dots, p + q + 1$) given by $f(\mathbf{w}_{\cdot j} | \mathbf{W}_{-j}, \mathbf{R}, \boldsymbol{\xi}_j)$. The proposed functional regression MICE (fregMICE), algorithm is provided in Algorithm 1. We assume that the variables are arranged such that those with the least missing data have lower index values (j) and those with the more missing data

have higher index values. As with the original MICE procedure, any pattern of missingness in the variables can be accommodated.

Algorithm 1 fregMICE Procedure for Imputation of Scalar and Functional Variables

- 1: Initialize the imputation procedure by filling in $\mathbf{w}_{\cdot j}^{mis}$ by a random draw from $\mathbf{w}_{\cdot j}^{obs}$ for each j .
Denote each initially complete $\mathbf{w}_{\cdot j}$ by $\mathbf{w}_{\cdot j}^{[0]}$.
 - 2: **for** v in $1, \dots, V$ **do**
 - 3: **for** j in $1, \dots, p + q + 1$ **do**
 - 4: **if** $\mathbf{w}_{\cdot j}$ has missing values **then**
 - 5: Set $\mathbf{D}_{-j}^{[v]} = (\mathbf{w}_{\cdot 1}^{[v]}, \mathbf{w}_{\cdot 2}^{[v]}, \dots, \mathbf{w}_{\cdot j-1}^{[v]}, \mathbf{w}_{\cdot j+1}^{[v-1]}, \dots, \mathbf{w}_{\cdot p+q+1}^{[v-1]})$. Let $\mathbf{D}_{-j}^{obs[v]}$ be the components in $\mathbf{D}_{-j}^{[v]}$ for which $\mathbf{w}_{\cdot j}$ are observed (having $n_{j,obs}$ observations) and $\mathbf{D}_{-j}^{mis[v]}$ be the components for which $\mathbf{w}_{\cdot j}$ are missing (having $n - n_{j,obs}$ observations).
 - 6: Draw a bootstrap sample of size $n_{j,obs}$, with replacement, from $\{\mathbf{D}_{-j}^{obs[v]}, \mathbf{w}_{\cdot j}^{obs}\}$ to obtain $\{\mathbf{D}_{-j}^{b,obs[v]}, \mathbf{w}_{\cdot j}^{b,obs}\}$.
 - 7: Using $\mathbf{w}_{\cdot j}^{b,obs}$ as the response and $\mathbf{D}_{-j}^{b,obs[v]}$ as the predictors fit (6) if $\mathbf{w}_{\cdot j}$ is a scalar or (7) if $\mathbf{w}_{\cdot j}$ is a function to obtain parameter estimates denoted by $\hat{\boldsymbol{\xi}}_j^{[v]}$.
 - 8: Predict $\mathbf{w}_{\cdot j}^{mis}$ by randomly drawing from the predictive distribution $f(\mathbf{w}_{\cdot j}^{mis} | \mathbf{D}_{-j}^{mis[v]}, \hat{\boldsymbol{\xi}}_j^{[v]})$ using methods described in Section 4.1.1. Fill the missing values of $\mathbf{w}_{\cdot j}$ with the predicted values. Set this completed vector to $\mathbf{w}_{\cdot j}^{[v]}$.
 - 9: **else** (when $\mathbf{w}_{\cdot j}$ is completely observed)
 - 10: Set $\mathbf{w}_{\cdot j}^{[v]} = \mathbf{w}_{\cdot j}$.
 - 11: When $v = V$, convergence is assumed. (Convergence is discussed in Section 4.1.3)
 - 12: Run this algorithm M times to obtain M complete data sets.
-

The fregMICE Algorithm can be run in parallel to produce the M streams/sequences that yield the M imputed data sets after V iterations.

4.1.3 Convergence and Diagnostics for the fregMICE Procedure

In settings with only scalar data, it is common to assess convergence of the MICE procedure via inspection of plots of selected parameters that summarize the imputed data (e.g., mean or standard deviation of the imputed values) vs. iteration number for each of the M parallel sequences. When the specified values for the parallel sequences are plotted together, the streams should overlap and be free of trend in order to diagnose convergence (van Buuren and Oudshoorn, 1999). We propose to use the same assessment techniques for imputations of scalar values generated from our fregMICE procedure and similar techniques for the im-

putations of functional values. More specifically, for the imputed function values, we propose to plot point-wise summary parameters (e.g., mean or standard deviation) vs. imputation number for each parallel sequence and will diagnose convergence if the plots are free of trend and show adequate overlap across the streams. We illustrate these plots and how to use them to assess convergence in our application of the fregMICE procedure in Section 6.

Aside from assessing convergence, one may also want to assess the fidelity of the imputed values to those observed in the data set. One way to do this is to create strip-plots. For imputed scalar data, these plots show the observed and imputed values from each imputed data set in contrasting colors. This allows one to easily identify whether imputed values are realistic and can help the analyst decide if the imputation model needs to be adjusted. Strip plots can also be constructed for imputed functional data and can be used to make similar assessments. We illustrate these plots in our application in Section 6.

4.2 Analysis of Multiply Imputed Datasets

The generation of multiple data sets accounts for the inherent uncertainty in the prediction of the missing values. Once the imputed data sets are constructed, we analyze each one using a method designed for complete data. Here that means that we use PFFR to estimate analysis model (1) when the response of interest is a function or PFR to estimate analysis model (2) when the response of interest is a scalar. The results from each fitted model on each of the M imputed data sets can be pooled to provide valid point estimates and variance estimates that account for both the within and between imputation variability. We propose to use the variance estimates to construct valid approximate confidence intervals for the scalar coefficients and point-wise confidence bands for the coefficient functions.

Rubin’s Rules (Rubin, 1987), which provide a way to combine scalar and multivariate estimates after MI, can be extended to cases involving both scalar and functional data. For clarity, we illustrate the pooling approach for parameters estimated in model (1). (Similar arguments can be made for model (2).) For model (1), fit on the m^{th} imputed data set, we

estimate $1 + p + q$ sets of parameters denoted by $\hat{\beta}_j^{(m)}(t) = \mathbf{B}_j^\top(t) \hat{\mathbf{b}}_j^{(m)}$ for $j = 0, \dots, p$ and $\hat{\rho}_k^{(m)}(s, t) = \mathbf{U}_k^\top(s, t) \hat{\mathbf{u}}_k^{(m)}$ for $k = 1, \dots, q$. With Q denoting the estimand of interest, let $Q(t) = \beta_j(t)$ and $\hat{Q}(t)$ be its estimator having sampling variance V that is estimated by \hat{V} . The estimator of Q based on the m -th completed data set is given by $\hat{Q}^{(m)}(t) = \mathbf{B}_j^\top(t) \hat{\mathbf{b}}_j^{(m)}$. We propose to use the pooled point estimate for $Q(t)$, based on the M imputed data sets given by $\bar{Q}_M(t) = \frac{1}{M} \sum_{m=1}^M \hat{Q}^{(m)}(t) = \frac{1}{M} \sum_{m=1}^M \mathbf{B}_j^\top(t) \hat{\mathbf{b}}_j^{(m)} = \mathbf{B}_j^\top(t) \left\{ \frac{1}{M} \sum_{m=1}^M \hat{\mathbf{b}}_j^{(m)} \right\} = \mathbf{B}_j^\top(t) \bar{\mathbf{b}}_{j,M}$.

As with Rubin's Rules for scalar and multivariate parameters, the total variance of $\bar{Q}_M(t)$ should incorporate both within and between imputation variability. Let $\hat{V}^{(m)}(t)$ be the variance of $\hat{Q}^{(m)}(t)$ from the m^{th} imputed data set. Hence we have $\hat{V}^{(m)}(t) = \widehat{\text{var}}\{\hat{Q}^{(m)}(t)\} = \widehat{\text{var}}\{\mathbf{B}_j^\top(t) \hat{\mathbf{b}}_j^{(m)}\} = \mathbf{B}_j^\top(t) \widehat{\text{var}}(\hat{\mathbf{b}}_j^{(m)}) \mathbf{B}_j(t) = \mathbf{B}_j^\top(t) \hat{\Lambda}_{\hat{\mathbf{b}}_j}^{(m)} \mathbf{B}_j(t)$, where $\hat{\Lambda}_{\hat{\mathbf{b}}_j}^{(m)}$ is the estimated covariance matrix of $\hat{\mathbf{b}}_j^{(m)}$. The `pffr` function from the `refund` package (Goldsmith *et al.*, 2018) can provide different estimates for the covariance matrix that are useful for constructing confidence intervals. In our simulations and application, we employ the Bayesian posterior covariance matrix (Ruppert *et al.*, 2003) which was also used in Ivanescu *et al.* (2015). With $\hat{V}^{(m)}(t)$ defined, we have that the mean within-imputation variance given by $\bar{V}_M(t) = \frac{1}{M} \sum_{m=1}^M \hat{V}^{(m)}(t) = \frac{1}{M} \sum_{m=1}^M \mathbf{B}_j^\top(t) \hat{\Lambda}_{\hat{\mathbf{b}}_j}^{(m)} \mathbf{B}_j(t) = \mathbf{B}_j^\top(t) \left\{ \frac{1}{M} \sum_{m=1}^M \hat{\Lambda}_{\hat{\mathbf{b}}}^{(m)} \right\} \mathbf{B}_j(t) = \mathbf{B}_j^\top(t) \bar{\Lambda}_{\hat{\mathbf{b}}_{j,M}} \mathbf{B}_j(t)$, and the between-imputation variability is given by

$$\begin{aligned} B_M(t) &= \frac{1}{M-1} \sum_{m=1}^M \left\{ \hat{Q}^{(m)} - \bar{Q}_M \right\}^2 = \frac{1}{M-1} \sum_{m=1}^M \left\{ \mathbf{B}_j^\top(t) \left(\hat{\mathbf{b}}_j^{(m)} - \bar{\mathbf{b}}_{j,M} \right) \right\}^2 \\ &= \mathbf{B}_j^\top(t) \left\{ \frac{1}{M-1} \sum_{m=1}^M \left(\hat{\mathbf{b}}_j^{(m)} - \bar{\mathbf{b}}_{j,M} \right)^\top \left(\hat{\mathbf{b}}_j^{(m)} - \bar{\mathbf{b}}_{j,M} \right) \right\} \mathbf{B}_j(t) \\ &= \mathbf{B}_j^\top(t) \bar{\mathbf{\Omega}}_{j,M} \mathbf{B}_j(t), \end{aligned}$$

where $\bar{\mathbf{\Omega}}_{j,M}$ is the covariance matrix quantifying the variability in the estimated basis coefficients between imputations. The total variance of $\bar{Q}_M(t)$ is then given by $\bar{V}_M(t) + (1 + \frac{1}{M})B_M(t)$, comprising contributions from variability within and between the imputed data sets. Recall that in the PFFR fitting procedure, the basis coefficients are viewed as random

effects each being normally distributed. Therefore we propose to construct approximate 95% confidence intervals for $Q(t_0)$ as $\bar{Q}_M(t_0) \pm 1.96\sqrt{\bar{V}_M(t_0) + (1 + \frac{1}{M})B_M(t_0)}$. We evaluate the performance of the approximate confidence intervals in a simulation study.

It is straightforward to construct similar pooled estimators and their corresponding variances for the bivariate coefficient functions $\rho_k^{(m)}(s, t)$ for $k = 1, \dots, q$ from the FRM. Similarly one can use the same procedures to obtain estimators and their corresponding variances for coefficient functions in a SRM if that is the analysis model of interest. In SRMs, one may also include scalar variables and their pooled estimators and corresponding variances can be computed using the standard methods proposed in Rubin (1987).

5 Simulation Study

The primary goal of our simulation study is to investigate the performance of the fregMICE procedure and to evaluate the characteristics of the pooled estimators and approximate confidence intervals proposed in the previous section. Though there are many possible settings we could have considered, the simulation results presented here were designed to be similar to the setting encountered in our application to the MDD data (i.e., relating a functional response to a set of scalar predictors when some of the data are missing). As there are no other methods in the literature to deal with this setting, we compare our fregMICE procedure to mean imputation and complete case analysis.

5.1 Data Generation

Our simulation study focuses on settings with a functional response, Y , and its association with three scalar predictors, Z_1, Z_2 , and Z_3 . We generated $Z_{1i} \sim \text{Bin}(1, 0.4)$ and $(Z_{2i}, Z_{3i}) \sim N((2, 0), \begin{pmatrix} 1 & 0.6 \\ 0.6 & 1 \end{pmatrix})$ for $i = 1, \dots, 350$. We selected $n = 350$ since this is close to the number of subjects in our application. The functional outcome is observed on a grid $\{t_g = \frac{g}{10} : g =$

$0, 1, \dots, 100\}$ on the interval $[0, 10]$ and related to the scalar predictors via the equation

$$Y_i(t) = \beta_0(t) + \beta_1(t)Z_{1i} + \beta_2(t)Z_{2i} + \beta_3(t)Z_{3i} + \varepsilon_i(t), \quad (8)$$

where we consider two sets of true coefficient functions. For the first set, which we refer to as “Parameter Set 1,” we have $\beta_0(t) = 0.25t$, $\beta_1(t) = \sin(\frac{\pi t}{10})$, $\beta_2(t) = 0.3e^{t/5}$, and $\beta_3(t) = -0.2\sin(\frac{\pi t}{10})$. For the second set, which we refer to as “Parameter Set 2,” we have $\beta_0(t) = 0.25t$, $\beta_1(t) = \sin(\frac{\pi t}{5})$, $\beta_2(t) = \frac{2}{\sqrt{2\pi}}e^{-(t-2)^2/2}$, $\beta_3(t) = \frac{-1}{\sqrt{2\pi}}\left\{e^{-(t-2)^2/2} + e^{-(t-8)^2/2}\right\}$. β_1, β_2 , and β_3 in Parameter Set 2 have more localized features relative to Parameter Set 1 and are therefore more challenging to estimate using the PFFR approach. In each setting, $\varepsilon_i(t)$ is simulated from a Gaussian process with mean zero and covariance $V(s, t) = 2^2 \cdot 0.15^{|s-t|} + 0.05^2 \cdot I(s = t)$ where $I(s = t)$ is 1 if $s = t$ and 0 otherwise. Figure 2 displays sets of simulated response functions generated under Parameter Sets 1 and 2.

Under each set of parameters, we consider two scenarios. In Scenario (a) only Z_2 has missing values and in Scenario (b) both Z_2 and Y have missing values. In both Scenarios (a) and (b), Z_1 and Z_3 are always fully observed and the probability that Z_2 is observed is given by $P(R_{Z_{2i}} = 1) = \alpha_0 - 20I\{S_i > \alpha_1\} + \alpha_2 \frac{1}{1+e^{-Z_{1i}}} + \alpha_3 \frac{1}{1+e^{-Z_{3i}}}$ for observation i where $S_i = \sum_{g=0}^{100} Y_i(t_g)$. In Scenario (a), where Y is always observed, we set $\alpha_0 = 10$, $\alpha_2 = \alpha_3 = 0$, and let α_1 be the 90th, 80th, or 70th percentile of $\{S_1, \dots, S_{350}\}$ so as to achieve 10%, 20%, or 30% missingness in Z_2 respectively. In Scenario (b), whether Z_2 is observed depends only upon the values of Z_1 and Z_3 such that $\alpha_1 = \max\{S_1, \dots, S_{350}\}$ (so that missingness is independent of Y), $\alpha_2 = 1$, $\alpha_3 = -1$ and $\alpha_0 = 2.1, 1.3$, or 0.8 to achieve 10%, 20%, or 30% missingness in Z_2 respectively. Also for Scenario (b), the probability that Y is observed is given by $P(R_{Y_i} = 1) = \psi_0 + \psi_1 \frac{1}{1+e^{-Z_{1i}}} + \psi_2 \frac{1}{1+e^{-Z_{3i}}}$ where $\psi_1 = -1$, $\psi_2 = 1$, and $\psi_0 = 2.3, 1.5$, or 0.9 to achieve 10%, 20%, or 30% missingness in Y respectively.

In Scenario (a), Z_2 values are MAR with missingness depending on the response, Y , in such a way that observations with missing data have functional responses that tend to have

larger values across the domain $[0,10]$. In this scenario, it is expected that complete case analysis will yield biased estimates. In Scenario (b), Z_2 values are MAR with missingness depending only on the other covariates, but not the response. The response, Y , is also MAR. In this scenario, complete case analysis is not expected to be biased. We generated 500 data sets under each parameter set/scenario/missingness combination.

5.2 Procedures Compared and Performance Measures

For each simulation setting, we fit the correctly specified model for Y and used four different procedures for handling missing data in order to make comparisons. Regardless of the procedure, the analysis model (8) was fit using PFFR where each coefficient function was represented via a basis set of 20 cubic B-splines and smoothness in the estimated coefficient functions was achieved via a penalty on the magnitude of the second derivative. As noted in Section 2.1, smoothing parameters were estimated via REML.

As a benchmark procedure, we used all of the data, prior to imposing missingness on any of the variables to fit model (8). We refer to this as “all no missing” (ANM). Second, we considered mean imputation. That is, we filled in any missing Z_2 values with the mean of the observed values of Z_2 and for missing Y functions, we filled in the point-wise mean function of the observed Y functions. We then used the mean-imputed dataset to fit model (8). The third procedure we considered was CCA where the analysis model was fit on observations with complete data only. Lastly, we considered our fregMICE procedure. The imputation model used for Z_2 was $E(Z_2|Z_1, Z_3, Y) = \gamma_0 + \gamma_1 Z_1 + \gamma_2 Z_3 + \int Y(t)\omega(t)dt$. To estimate this model, we used PFR. In the PFR fitting procedure, functional observations were represented using functional principal components (FPCs) by smoothed covariance (Yao *et al.*, 2003) where the number of FPCs was selected to be the minimum number of components explaining at least 99% of the variance in the functional observations. The coefficient function, ω , was represented using a basis of 30 thin-plate regression splines and the fitting procedure penalized the magnitude of the second derivative. In scenarios where

Y had missing values, the imputation model for Y was the same as (8). To estimate this model, we used the correctly specified analysis model fit via PFFR, using 20 cubic B-splines to represent each coefficient function and penalized the magnitude of the second derivative. We ran the fregMICE procedure for 20 iterations and constructed 5 imputed data sets. We fit model (8) on each imputed data set and used the extension of Rubin’s rules described in Section 4.2 to pool estimates from the 5 data sets.

Procedures were compared with respect to several performance measures of the estimates $\hat{\beta}_j(t)$ for $j = 0, 1, 2$, and 3. In addition to providing plots of point-wise mean (pwM) estimates for each coefficient function, we also provide point-wise standardized bias (pwSB). The pwSB was calculated as $SB(t_g) = \frac{\bar{\hat{\beta}}_j(t_g) - \beta_j(t_g)}{sd\{\hat{\beta}_j(t_g)\}}$, where $\bar{\hat{\beta}}_j(t_g)$ is the average of the 500 estimates of $\beta_j(t_g)$ and $sd\{\hat{\beta}_j(t_g)\}$ is the Monte-Carlo standard deviation of the estimates. As a global measure of estimation performance for each coefficient function, we computed the mean integrated squared error (MISE) which we calculated as $MISE(\hat{\beta}_j) = \frac{1}{500} \sum_{v=1}^{500} \int_0^{10} \{\hat{\beta}_{j,v}(t) - \beta_j(t)\}^2 dt$, where $\hat{\beta}_{j,v}(t)$ is the estimate of $\beta_j(t)$ in the v^{th} simulated data set. Point-wise coverage (pwCov) and point-wise width (pwWidth) of the 95% point-wise confidence intervals are provided in the Supplementary Materials while here we report global measures of across-the-function coverage and width for each coefficient function by taking the mean coverage and width, respectively, over all t_g values and then averaging over the 500 simulation runs.

5.3 Results

5.3.1 Setting 1 Results

Scenario (a): Figure 3 shows the pwM (top panels) and pwSB (bottom panels) for Parameter Set 1 Scenario (a). The pwM and pwSB for estimates derived from our fregMICE procedure tend to be comparable to those derived from ANM while estimates derived from CCA and after mean imputation show bias for each coefficient function even though data are only missing for the Z_2 variable. Since missingness of Z_2 depends on the functional response, we expected CCA to result in biased estimates for the coefficient functions. We note that

the degree of bias is considerably greater when the mean imputation procedure is employed. The degree of bias in estimates derived from both CCA and after mean imputation increases as the amount of missing data increases. Across-the-function MISE values are provided in Section 1 of the Supplementary Materials and reinforce the superior performance of the fregMICE procedure over mean imputation and CCA. Mean pwCov and pwWidth are shown in the top half of Table 1. With respect to coverage, the fregMICE procedure is comparable to ANM, though the intervals tend to be slightly wider, especially as the amount of missing data increases. The coverage rate decreases substantially and width increases slightly for intervals for β_2 from CCA and mean imputation as the amount of missing data increases. Coverage is extremely poor for intervals derived via the mean imputation procedure. Plots of the pwCov and pwWidth are provided in Appendix Section 1.

Scenario (b): Figure 4 shows the pwM (top panels) and pwSB (bottom panels) for Parameter Set 1 Scenario (b). Again, the estimates derived from fregMICE procedure perform comparably to ANM. Estimates derived from CCA tend to perform comparably as well. This is expected since missingness in both Y and Z_2 only depends on the completely observed covariates, Z_1 and Z_3 . Inspection of the MISE values (in Section 1 of the Supplementary Material) reveals that fregMICE is slightly superior to CCA as it tends to show smaller MISE values for each coefficient function for all amounts of missingness. Estimates derived from mean imputation perform poorly. Mean pwCov and pwWidth are shown in the bottom half of Table 1 and display similar performance for the ANM, CCA, and fregMICE procedures. In all settings, fregMICE shows either slightly better coverage than CCA or comparable coverage and narrower width. Coverage is very poor for intervals derived from mean imputation. Plots of the pwCov and pwWidth are provided in Appendix Section 1.

5.3.2 Setting 2 Results

Scenario (a): Figure 5 shows the pwM (top panels) and pwSB (bottom panels) for Parameter Set 2 Scenario (a). The pwM and pwSB for estimates derived from the fregMICE

procedure are comparable to those derived from ANM. Estimates derived from CCA and after mean imputation show bias for each coefficient function - neither procedure is uniformly better than the other, with CCA estimates showing less bias than mean imputation over some regions of the domain (for some coefficient functions) while the opposite is true over other regions of the domain. For example, with 30% missing data in Z_2 , the magnitude of the pwSB for β_2 is larger for mean imputation than for CCA over values of t in the interval $[0, 3.75)$, but the magnitude is smaller over values of t in the interval $(3.75, 10]$ and the opposite holds for estimates of β_3 with 30% missingness. Across-the-function MISE values are provided in Appendix Section 1 and reinforce the superior performance of the fregMICE procedure. Mean pwCov and pwWidth are shown in the top half of Table 2. With respect to coverage, the fregMICE procedure is comparable to ANM, though the intervals tend to be slightly wider, especially as the amount of missing data increases. The coverage rate decreases and the intervals' width increases for β_2 and β_3 from CCA and mean imputation as the amount of missing data increases. The interval coverages and widths corresponding to β_1 , the coefficient for binary Z_1 that is always observed, are similar for all procedures. Plots of the pwCov and pwWidth are provided in Appendix Section 1.

Scenario (b): Figure 6 shows the pwM (top panels) and pwSB (bottom panels) for Parameter Set 2 Scenario (b). Again, the estimates derived from fregMICE procedure perform comparably to ANM. Estimates derived from CCA tend to perform comparably well. As discussed above, this is expected since missingness in both Y and Z_2 only depends on the completely observed covariates, Z_1 and Z_3 . Inspection of the MISE values (Appendix Section 1) reveals that fregMICE is slightly superior to CCA as it tends to show smaller MISE values for each coefficient function across all amounts of missingness. Estimates derived from mean imputation perform very poorly. Mean pwCov and pwWidth are shown in the bottom half of Table 2 and display similar performance for the ANM, CCA, and fregMICE procedures. In all settings, fregMICE shows either slightly better coverage than CCA or comparable coverage and narrower width. Coverage is very poor for intervals from mean imputed data.

Plots of the pwCov and pwWidth are provided in Appendix Section 1.

5.3.3 Results Summary

In summary, with respect to bias and coverage of point-wise confidence intervals, the fregMICE procedure tends to perform comparably to the best case scenario where all data are available and at least as well as or much better than CCA and mean imputation. Though CCA should be unbiased in settings where missingness is independent of the outcome, fregMICE still tends to perform as well or slightly better on the reported performance measures. Across all settings, mean imputation performs very poorly in all respects. Performance measures deteriorate substantially with increasing amounts of missingness. Accordingly, we do not recommend using mean imputation to handle missing data in the functional regression setting and given the availability of software for fregMICE, CCA should also be avoided.

6 Application to EMBARC Data

In Section 1 we stated that our goal is to use the EMBARC data to characterize the association between FA and MDD status. van der Vinne *et al.* (2017) suggest that analysis of FA should adjust for age and gender and consider their potential modifying effects. In our model, we decided to only include the main effect of age since van der Vinne *et al.* (2017) found that dichotomized age (< 53 vs. ≥ 53) acts as an effect modifier of the association between FA and depression status, but most of the subjects in the EMBARC data set are younger than 53. In addition to considering age and gender, Kaiser *et al.* (2018) suggest controlling for handedness (left vs. right) and cognition (mental ability). We follow these suggestions in formulating the following functional response analysis model:

$$FA_i(t) = \beta_0(t) + AGE_i\beta_1(t) + EHI_i\beta_2(t) + WASIV_i\beta_3(t) + MDD_i\beta_4(t) + SEX_i\beta_5(t) + MDD_i*SEX_i\beta_6(t) + \varepsilon_i(t). \quad (9)$$

In model (9) FA_i are the normalized CSD asymmetry curves for $i = 1, \dots, 335$ shown in Figure 1 for those subjects with “Good” or “Acceptable” quality designations. AGE_i is age in years, EHI_i is the score for the Edinburgh Handedness Inventory ranging from -100 to 100 (-100 corresponds to being completely left-handed and 100 corresponds to being completely right-handed), $WASIV_i$ is the raw score for the verbal component of the Wechsler Abbreviated Scale of Intelligence (a measure of cognitive ability with higher values indicating better performance; values range from 20 to 80), MDD_i is binary indicating disease status ($1 = \text{MDD}$, $0 = \text{HC}$), and SEX_i is binary ($1 = \text{Female}$, $0 = \text{Male}$).

Table 3 shows summary statistics and number of observations available for the variables in the model. The scalar predictor WASIV is missing for 49 of the 335 subjects. EEG data are completely missing for 11 subjects. Among the remaining 324 subjects with EEG data available, 88 have data that are deemed “Marginal” or “Unacceptable.” We will not use these poor-quality EEG data in our analysis.

A CCA approach for fitting model (9) will use 204 (60.9%) complete observations. As an alternative, we used our newly proposed fregMICE method to impute the missing WASIV scores and the missing and poor-quality FA functions. For maximal flexibility, we imputed the missing values separately within the HC ($n_{HC} = 40$) and MDD ($n_{MDD} = 295$) groups of subjects. Due to limited sample size, we chose not to further split the sample by sex in each diagnostic group for the purpose of imputation. The imputation model for the WASIV scores had the same form given in (6) using all the other variables specified in the analysis model (9) as the predictors as well as QIDS score (a measure of depressive symptomatology that was available for all HC and MDD subjects). We employed PFR to fit the WASIV imputation model and used the similar settings outlined in Section 5.2 for basis functions and penalization. The only difference here is that we chose to represent the unknown coefficient functions with a set of 30 B-spline basis functions. The imputation model for the FA functions was model (9) with the additional QIDS score predictor. We employed PFFR to fit the FA imputation model and used the same settings outlined in

Section 5.2 for basis functions and penalization. We generated 20 imputed data sets by running the fregMICE Algorithm for 20 iterations to obtain each imputed data set.

Figure 7 shows diagnostic plots of the mean value of the imputed WASIV scores at each iteration of the fregMICE algorithm for each of the 20 streams (various line colors) in the HC and MDD subsets. We see a fair amount of mixing in the streams and no discernible patterns that would suggest convergence issues with respect to the WASIV imputed values. Strip plots showing the imputed and observed values for the the WASIV scores from each of the 20 imputed data sets are provided in Figure 8. These plots reveal several instances when the imputed WASIV scores were higher than the maximum possible score of 80. This occurred for several imputed values in the MDD and HC subsets. Any values that were predicted to be greater than 80 were set to 80 prior to fitting the analysis model.

Figure 9 shows plots of the mean functional values of the imputed FA curves at each iteration of the fregMICE algorithm for each of the 20 streams (different curve colors) in the HC and MDD subsets. Note that we have scaled the horizontal axis values to be between 0 and 1. Again, we see a fair amount of mixing in the streams and no discernible patterns that would suggest convergence issues with respect to the FA imputed values. Strip plots showing the imputed and observed values for the the FA functions from each of the 20 imputed data sets are provided in Appendix Section 2. These plots reveal that the imputed FA functions tend to fall within the range of values of the observed FA functions and have similar characteristics. Imputed function values needed no adjustments.

We combined the m^{th} imputed data set for the HC subset with the m^{th} imputed data set for the MDD subset for $m = 1, \dots, 20$ to obtain the 20 complete imputed data sets. We fit model (9) on each of the 20 complete imputed data sets via PFFR using the same settings as the imputation model for the FA curves described above. Results were pooled and approximate 95% point-wise confidence bands were calculated according to Section 4.2.

Figure 10 shows the pooled functional coefficient estimates and corresponding 95% point-wise confidence bands for model (9) as well as estimates and confidence bands derived from

CCA and after mean imputation. Though it is clear that the pooled coefficient estimates derived from the fregMICE imputed data sets are different from the estimated coefficients derived from the other methods, the widths of the 95% confidence bands make it difficult to claim that the different methods lead to very different conclusions.

Since primary interest lies in understanding the relationship between FA, depression status, and gender, the focus of inference lies in the functional coefficient estimates corresponding to the MDD ($\hat{\beta}_4$), SEX ($\hat{\beta}_5$), and MDD \times SEX ($\hat{\beta}_6$) variables. Specifically, assessing the association between FA and depression status in males is equivalent to testing the null hypothesis $H_0 : \beta_4(t) = 0 \ \forall \ t$. Rather than derive a p-value, we can use the approximate 95% point-wise confidence band to see that, regardless of which method is used, the confidence band for $\hat{\beta}_4(t)$ (corresponding to the MDD panel in Figure 10) does not contain 0 for frequencies greater than about 6 Hz (mid theta, alpha, and beta bands). $\hat{\beta}_4(t)$ suggests that males with MDD have greater left than right CSD power (since the curve takes on negative values) with the largest differences in the beta band (16 - 32 Hz). Assessing the association between FA and depression status in females is equivalent to testing the null hypothesis $H_0 : \beta_4(t) + \beta_6(t) = 0 \ \forall \ t$. The estimate, $\hat{\beta}_4(t) + \hat{\beta}_6(t)$ and its corresponding point-wise confidence band are not shown here, but suggest that there is little to no difference in FA, particularly in the alpha band, comparing females with MDD to female HCs. Alternatively, we can view the model-based mean FA curves for different combinations of the predictor values. We have created a Shiny app, available in the Supplementary Materials, to do this. Figure 11 shows one set of plots that can be obtained from the Shiny app in which we plot the mean FA curves for male and female MDD and HC subjects whose covariates are set to the mean values in the data set (i.e., AGE = 37.16, EHI = 71.48, and WASIV = 64.08). This plot reveals clear differences between males and females with respect to the association between FA (across the entire range of frequencies) and depression status specifically when we use the fregMICE procedure to impute the missing data. All together, these results suggest that FA, primarily in the alpha and beta bands, may be useful as a biomarker for

depression in males, but not in females.

Inspection of the estimates from each of the 20 imputed data sets (not shown here) reveals that the wide widths of the confidence bands around the coefficient estimates and predicted mean curves based on the fregMICE procedure are due to the relatively large amount of between imputation variance. This is not surprising considering that imputation was conducted separately for the HC and MDD samples where the HC sample had a small sample size of 40. Estimates from the 20 imputed data sets show that the predicted mean FA curves for male HC subjects were consistently higher than the curves for male MDD subjects while the mean FA curves for female HC subjects were at or below the curves for female MDD subjects in 14 of the 20 imputed data sets.

7 Discussion

Research on how to handle incomplete data in the framework of functional data analysis is extremely limited although there are some exceptions. For example, Febrero-Bande *et al.* (2019) consider approaches for handling missing scalar responses in scalar-on-function regression models, while Preda *et al.* (2009) and (He *et al.*, 2011) consider settings where the functional data are missing over part of their domain. However, none of these approaches are applicable in settings like the one that motivates our work, where an entire functional value is missing for some observations. To our knowledge, the current state-of-the-art for handling missing data in functional regression with missing functional data is to simply ignore the missing data and perform a complete case analysis. As in the purely scalar setting, complete case analysis is not a universally acceptable approach. In this article, we extended the MICE algorithm to perform multiple imputation with missing data that are scalar or function-valued and extended Rubin’s Rules to provide valid parameter estimates and standard errors. Our simulations, which focus on functional response model estimation, show that, in some settings, complete case analysis can lead to biased estimates for the param-

eters of interest and correspondingly poor coverage for point-wise confidence bands. Mean imputation also often performs extremely poorly.

We applied the proposed set of methods to conduct an analysis of the association between frontal CSD power asymmetry and depression status in subjects from the EMBARC study, some having missing values on relevant variables. Since the CSD power asymmetry response is a function, we fit a functional response model that was estimated using penalized functional regression. Analyses using the newly proposed methods revealed that, adjusting for age, handedness, and cognitive ability, males with depression tend to have higher left than right frontal CSD power across a wide range of frequency values ($\sim 6 - 31$ Hz) while there was no evidence of a difference between female depressed subjects and healthy controls with respect to frontal asymmetry. This suggests that frontal asymmetry in the mid-theta, alpha, and beta bands may be able to serve as a biomarker for depression in males. Common analyses of frontal asymmetry in relation to depression are often conducted after CSD power asymmetry has been reduced to a single scalar summary (e.g., mean frontal alpha asymmetry). Taking a functional data analytic approach allows one to gain insight about the relationship between frontal CSD power asymmetry and depression that cannot be captured by the commonly-employed approach. By modeling frontal CSD power across a wide range of frequency values, we give ourselves the ability to determine if the relationship changes across the range of frequencies. Furthermore, by conducting the functional data analysis first, we can determine whether reducing CSD power asymmetry curves to aggregate scalar summaries is justified.

Though motivated by our need to fit a functional response model on EEG data, the fregMICE method paired with the extension of Rubin’s Rules to functional data comprises a set of tools that can be applied to both functional and scalar response models with both scalar and/or functional predictors. Since we chose to employ PFR and PFFR fitting procedures, the fregMICE method can be extended to handle sparsely sampled functional data, functional data that are not observed on the same grid-points, or functional data that are observed with noise. We believe that the fregMICE method and subsequent modifications of the algorithm

will be valuable tools as functional data are increasingly incorporated into modern studies.

We consider the methods presented here as an early step towards assembling a collection of tools to judiciously handle incomplete functional data in the context of fitting functional regression models. The proposed extensions to existing multiple imputation methods do have several limitations. First, as in the completely scalar case, the MAR assumption should hold in order for the the proposed methods to yield unbiased estimates of the parameters of interest. Potthoff *et al.* (2006) discuss this issue and propose techniques for assessing the MAR assumption which are applicable in the present context. For MNAR cases, more complex imputation models which include joint modeling of data and missingness are needed. Second, it is clear that the imputation models should be specified so as to provide high-quality imputations. This becomes a complex task, with respect to both correct/adequate specification and computation, in settings with many scalar and functional variables. Such settings will be prevalent as the trajectory of medical and public health research suggests that studies will be collecting greater amounts of both types of variables. This will be further complicated in studies where higher dimensional functional objects are included (e.g., two or three-dimensional images, etc.). New robust and computationally efficient methods will need to be developed to handle missing data in such settings. Third, as we noted in Section 4.1.3, checking convergence of the standard MICE procedure tends to rely on ad hoc approaches like inspection of various convergence plots of summary measures. While we employed a similar approach in our application via plotting the point-wise mean of the imputed functions at each iteration, it may be instructive to consider other summary measures (e.g., cross-covariance, measures of smoothness, etc.) to assess convergence for those models that impute missing functional data. The development of rigorous convergence diagnostics could be the focus of valuable future research. Lastly, we applied normal approximations in constructing the confidence bands around the functional parameters using our extension of Rubin’s Rules. Such approximations are common in the functional regression literature (Goldsmith *et al.*, 2011; Ivanescu *et al.*, 2015), but it is possible that the confidence bands

could have better performance with respect to coverage and width if critical values based on a t-distribution with the appropriate degrees of freedom is used. Future research will investigate how to derive the correct degrees of freedom for t-distributions in such applications.

Supplementary Materials

`fregMICE_Appendix.pdf` provides additional simulation results in Section 1 and the functional strip plots for the FA curves from the application in Section 2. The zip file `Model-Based_FA_Shiny_App.zip` contains the Shiny app described in Section 6. R code for implementing the fregMICE procedure and the simulations in Section 5 are available in the zip file `fregMICE_R_Code.zip`.

References

- American Psychiatric Association (2013). *Diagnostic and statistical manual of mental disorders (5th ed.)*. American Psychiatric Association, Washington, DC.
- Bapna, R., Jank, W., and Shmueli, G. (2008). Price formation and its dynamics in online auctions. *Decision Support Systems* **44**:641 – 656.
- Bartlett, J., Carpenter, J., Tilling, K., and Vansteelandt, S. (2014). Improving upon the efficiency of complete case analysis when covariates are mnar. *Biostatistics* **15**:719 – 730.
- Besse, P., Cardot, H., Faivre, R., and Goulard, M. (2005). Statistical modelling of functional data. *Applied Stochastic Models in Business and Industry* **21**:165 – 173.
- Buckner, R., Head, D., Parker, J., Fotenos, A., Marcus, D., Morris, J., and Snyder, A. (2004). A unified approach for morphometric and functional data analysis in young, old, and demented adults using automated atlas-based head size normalization: reliability and validation against manual measurement of total intracranial volume. *NeuroImage* **23**:724 – 738.

- Burgette, L. and Reiter, J. (2010). Multiple imputation for missing data via sequential regression trees. *American Journal of Epidemiology* **172**:1070 – 1076.
- Buuren, S. and Groothuis-Oudshoorn, K. (2011). mice: Multivariate imputation by chained equations in r. *Journal of Statistical Software* **45**:1 – 67.
- Cardot, H., Ferraty, F., and Sarda, P. (1999). Functional linear model. *Statistics & Probability Letters* **45**:11 – 22.
- Ciarleglio, A., Petkova, E., Ogden, R., and Tarpey, T. (2015). Treatment decisions based on scalar and functional baseline covariates. *Biometrics* **71**:884 – 894.
- Collins, L., Schafer, J., and Kam, C. (2001). A comparison of inclusive and restrictive strategies in modern missing data procedures. *Psychological Methods* **6**:330 – 351.
- Crainiceanu, C., Staicu, A., and Di, C. (2009). Generalized multilevel functional regression. *Journal of the American Statistical Association* **104**:1550 – 1561.
- Crambes, C., Kneip, A., and Sarda, P. (2009). Smoothing spline estimators for functional linear regression. *Annals of Statistics* **37**:35 – 72.
- Doove, L., van Buuren, S., and Dusseldorp, E. (2014). Recursive partitioning for missing data imputation in the presence of interaction effects. *Computational Statistics and Data Analysis* **72**:92 – 104.
- Erbas, B., Akram, M., Gertig, D., English, D., Hopper, J., Kavanagh, A., and Hyndman, R. (2010). Using functional data analysis models to estimate future time trends in age-specific breast cancer mortality for the united states and england-wales. *Journal of Epidemiology* **20**:159 – 165.
- Faraway, J. (1997). Regression analysis for a functional response. *Technometrics* **39**:254 – 261.

- Febrero-Bande, M., Galeano, P., and González-Monteiga, W. (2019). Estimation, imputation and prediction for the functional linear model with scalar response with responses missing at random. *Computational Statistics and Data Analysis* **131**:91–103.
- Gao, H. and Niemeier, D. (2008). Using functional data analysis of diurnal ozone and NOx cycles to inform transportation emissions control. *Transportation Research Part D: Transport and Environment* **13**:221 – 238.
- Gertheiss, J., Goldsmith, J., Crainiceanu, C., and Greven, S. (2013). Longitudinal scalar-on-functions regression with application to tractography data. *Biostatistics* **14**:447 – 461.
- Goldsmith, J., Bobb, J., Crainiceanu, C., and Reich, D. (2011). Penalized functional regression. *Journal of Computational and Graphical Statistics* **20**:830–851.
- Goldsmith, J., Scheipl, F., Huang, L., Wrobel, J., Gellar, J., Harezlak, J., McLean, M., Swihart, B., Xiao, L., Crainiceanu, C., and Reiss, P. (2018). *refund: Regression with Functional Data. R package version 0.1-17*.
- Guo, W. (2002). Functional mixed effect models. *Biometrics* **53**:121 – 128.
- Harel, O., Perkins, N., and Schisterman, E. (2014). The use of multiple imputation for data subject to limits of detection. *Sri Lankan Journal of Applied Statistics* **5**:227 – 246.
- Harel, O. and Zhou, X.-H. (2007). Multiple imputation: Review of theory, implementation and software. *Statistics in Medicine* **26**:3057 – 3077.
- Harezlak, J., Wu, M., Wang, M., Schwartzman, A., Christiani, D., and Lin, X. (2008). Biomarker discovery for arsenic exposure using functional data. analysis and feature learning of mass spectrometry proteomic data. *Journal of Proteome Research* **7**:217 – 224.
- He, Y., Yucel, R., and Raghunathan, T. E. (2011). A functional multiple imputation approach to incomplete longitudinal data. *Statistics in Medicine* **30**:1137–1156.

- Henderson, B. (2006). Exploring between site differences in water quality trends: a functional data analysis approach. *Environmetrics* **17**:65 – 80.
- Honaker, J., King, G., and Blackwell, M. (2011). Amelia II: A program for missing data. *Journal of Statistical Software* **45**:1 – 47.
- Hutchinson, R., McLellan, P., Ramsay, J., Sulieman, H., and Bacon, D. (2004). Investigating the impact of operating parameters on molecular weight distributions using functional regression. *Macromolecular Symposia* **206**:495 – 508.
- Ikeda, T., Dowd, M., and Martin, J. (2008). Application of functional data analysis to investigate seasonal progression with interannual variability in plankton abundance in the bay of fundy, canada. *Estuarine, Coastal and Shelf Science* **78**:445 – 455.
- Ivanescu, A. E., Staicu, A.-M., Scheipl, F., and Greven, S. (2015). Penalized function-on-function regression. *Computational Statistics* **30**:539–568.
- J. O. Ramsay, B. R. (2002). Functional data analysis of the dynamics of the monthly index of nondurable goods production. *Journal of Econometrics* **107**:327 – 344.
- James, G. (2002). Generalized linear models with functional predictors. *Journal of the Royal Statistical Society, Series B* **64**:411 – 432.
- James, G., Wang, J., and Zhu, J. (2009). Functional linear regression that’s interpretable. *Annals of Statistics* **37**:2083 – 2108.
- Jank, W. and Shmueli, G. (2006). Functional data analysis in electronic commerce research. *Statistical Science* **21**:155 – 166.
- Kaiser, A., Gnjezda, M., Knasmüller, S., and Aichhorn, W. (2018). Electroencephalogram alpha asymmetry in patients with depressive disorders: current perspectives. *Neuropsychiatric Disease and Treatment* **14**:1493 – 1504.

- Little, R. and Rubin, D. (2002). *Statistical Analysis with Missing Data*. Wiley.
- Maronna, R. and Yohai, V. (2013). Robust functional linear regression based on splines. *Computational Statistics and Data Analysis* **65**:46 – 55.
- Marx, B. and Eilers, P. (1999). Generalized linear regression on sampled signals and curves: A P-spline approach. *Technometrics* **41**:1 – 13.
- McCullagh, P. and Nelder, J. (1989). *Generalized Linear Models*. Chapman and Hall/CRC.
- McLean, M., Hooker, G., Staicu, A., Scheipl, F., and Rupert, D. (2014). Functional generalized additive models. *Journal of Computational and Graphical Statistics* **23**:249 – 269.
- Meng, X. (1994). Multiple imputation inferences with uncongenial sources of input. *Statistical Science* **9**:538 – 558.
- Morris, J. and Carroll, R. (2006). Wavelet-based functional mixed models. *Journal of the Royal Statistical Society, Series B* **68**:179 – 199.
- Ogden, R., Miller, C., Takezawa, K., and Ninomiya, S. (2002). Functional regression in crop lodging assessment with digital images. *Journal of Agricultural, Biological, and Environmental Statistics* **7**:389 – 402.
- Perkins, N., Cole, S., Harel, O., Tchetgen, E. T., Sun, B., Mitchell, E., and Schisterman, E. (2018). Principled approaches to missing data in epidemiologic studies. *American Journal of Epidemiology* **187**:568 – 575.
- Potthoff, R., Tudor, G., Peiper, K., and Hasselblad, V. (2006). Can one assess whether missing data are missing at random in medical studies? *Statistical Methods in Medical Research* **15**:231 – 234.

- Preda, C., Saporta, G., Hedi, M., and Mbarek, B. H. (2009). The NIPALS algorithm for missing functional data. In *Proceedings of the 6th International Conference on Partial Least Squares and Related Methods*.
- R Development Core Team (2018). R: A language and environment for statistical computing. R Foundation for Statistical Computing. Vienna, Austria.
- R. T. Ogden, E. G. (2010). Wavelet modeling of functional random effects with application to human vision data. *Journal of Statistical Planning and Inference* **140**:3797 – 3808.
- Ramsay, J. O. and Silverman, B. W. (2005). *Functional Data Analysis, Second Edition*. Springer, New York.
- Ratcliffe, S., Leader, L., and Heller, G. (2002a). Functional data analysis with application to periodically stimulated foetal heart rate data. i: functional regression. *Statistics in Medicine* **21**:1103 – 1114.
- Ratcliffe, S., Leader, L., and Heller, G. (2002b). Functional data analysis with application to periodically stimulated foetal heart rate data. ii: functional logistic regression. *Statistics in Medicine* **21**:1115 – 1127.
- Reiss, P. and Ogden, R. (2007). Functional principal component regression and functional partial least squares. *Journal of the American Statistical Association* **102**:984 – 996.
- Reiss, P. and Ogden, R. (2010). Functional generalized linear models with images as predictors. *Biometrics* **66**:61 – 69.
- Rubin, D. (1987). *Multiple Imputation in Nonresponse Surveys*. John Wiley & Sons, Ltd.
- Ruppert, D., Wand, M., and Carroll, R. (2003). *Semiparametric Regression*. Cambridge University Press, Cambridge.
- SAS Institute Inc (2011). Sas/stat software version 9.3. <http://www.sas.com/>.

- Schafer, J. (1997). *Analysis of Incomplete Multivariate Data*. Chapman & Hall, London.
- Scheipl, F., Staicu, A., and Greven, S. (2015). Functional additive mixed models. *Journal of Computational and Graphical Statistics* **24**:477 – 501.
- Sørensen, H., Goldsmith, J., and Sangalli, L. (2013). An introduction with medical applications to functional data analysis. *Statistics in Medicine* **32**:5222 – 5240.
- Stewart, K., Darcy, D., and Daniel, S. (2006). Opportunities and challenges applying functional data analysis to the study of open source software evolution. *Statistical Science* **21**:167 – 178.
- Tenke, C., Kayser, J., Manna, C., Fekri, S., Kroppmann, C., Schaller, J., Alschuler, D., Stewart, J., McGrath, P., and Bruder, G. (2011). Current source density measures of electroencephalographic alpha predict antidepressant treatment response. *Biological Psychiatry* **70**:388 – 394.
- Tenke, C., Kayser, J., Pechtel, P., Webb, C., Dillon, D., Goer, F., Murray, L., Deldin, P., Kurian, B., McGrath, P., Parsey, R., Trivedi, M., Fava, M., Weissman, M., McInnis, M., Abraham, K., Alvarenga, J., Alschuler, D., Cooper, C., Pizzagalli, D., and Bruder, G. (2017). Demonstrating test-retest reliability of electrophysiological measures for healthy adults in a multisite study of biomarkers of antidepressant treatment response. *Psychophysiology* **54**:34 – 50.
- Torres, J., Nieto, P. G., Alejano, L., and Reyes, A. (2011). Detection of outliers in gas emissions from urban areas using functional data analysis. *Journal of Hazardous Materials* **186**:144 – 149.
- Trivedi, M. H., McGrath, P. J., Fava, M., Parsey, R. V., Kurian, B. T., Phillips, M. L., Oquendo, M. A., Bruder, G., Pizzagalli, D., Toups, M., Cooper, C., Adams, P., Weyandt, S., Morris, D. W., Grannemann, B. D., Ogden, R. T., Buckner, R., McInnis, M., Kraemer,

- H. C., Petkova, E., Carmody, T. J., and Weissman, M. M. (2016). Establishing moderators and biosignatures of antidepressant response in clinical care (EMBARC): Rationale and design. *Journal of Psychiatric Research* **78**:11 – 23.
- van Buuren, S. (2012). *Flexible Imputation of Missing Data*. CRC Press.
- van Buuren, S. and Oudshoorn, K. (1999). Flexible multivariate imputation by MICE. Technical report, TNO Prevention Center, Leiden, The Netherlands.
- van der Vinne, N., Vollebregt, M., van Putten, M., and Arns, M. (2017). Frontal alpha asymmetry as a diagnostic marker in depression: Fact or fiction? A meta-analysis. *Neuroimage: Clinical* **16**:79–87.
- White, I. and Carlin, J. (2010). Bias and efficiency of multiple imputation compared with complete-case analysis for missing covariate values. *Statistics in Medicine* **29**:2920 – 2931.
- White, I., Royston, P., and Wood, A. (2011). Multiple imputation using chained equations: Issues and guidance for practice. *Statistics in Medicine* **30**:377 – 399.
- Xu, D., Daniels, M., and Winterstein, A. (2016). Sequential BART for imputation of missing covariates. *Biostatistics* **17**:589 – 602.
- Yao, F., Müller, H., Clifford, A., Dueker, S., Follett, J., Lin, Y., Buchholz, B., and Vogel, J. (2003). Shrinkage estimation for functional principal component scores with application to the population. *Biometrics* **59**:676 – 685.
- Yao, F., Müller, H., and Wang, J. (2005). Functional linear regression for longitudinal data. *Annals of Statistics* **33**:2873 – 2903.
- Zahid, F. and Heumann, C. (2018). Multiple imputation with sequential penalized regression. *Statistical Methods in Medical Research* **5**:1311 – 1327.
- Zhao, Y. and Long, Q. (2016). Multiple imputation in the presence of high dimensional data. *Statistical Methods in Medical Research* **25**:2021 – 2035.

- Zhao, Y., Ogden, R., and Reiss, P. (2012). Wavelet-based LASSO in functional linear regression. *Journal of Computational and Graphical Statistics* **21**:600 – 617.
- Zhu, H., Yao, F., and Zhang, H. (2014). Structured functional additive regression in reproducing kernel Hilbert spaces. *Journal of the Royal Statistical Society, Series B* **76**:581 – 603.

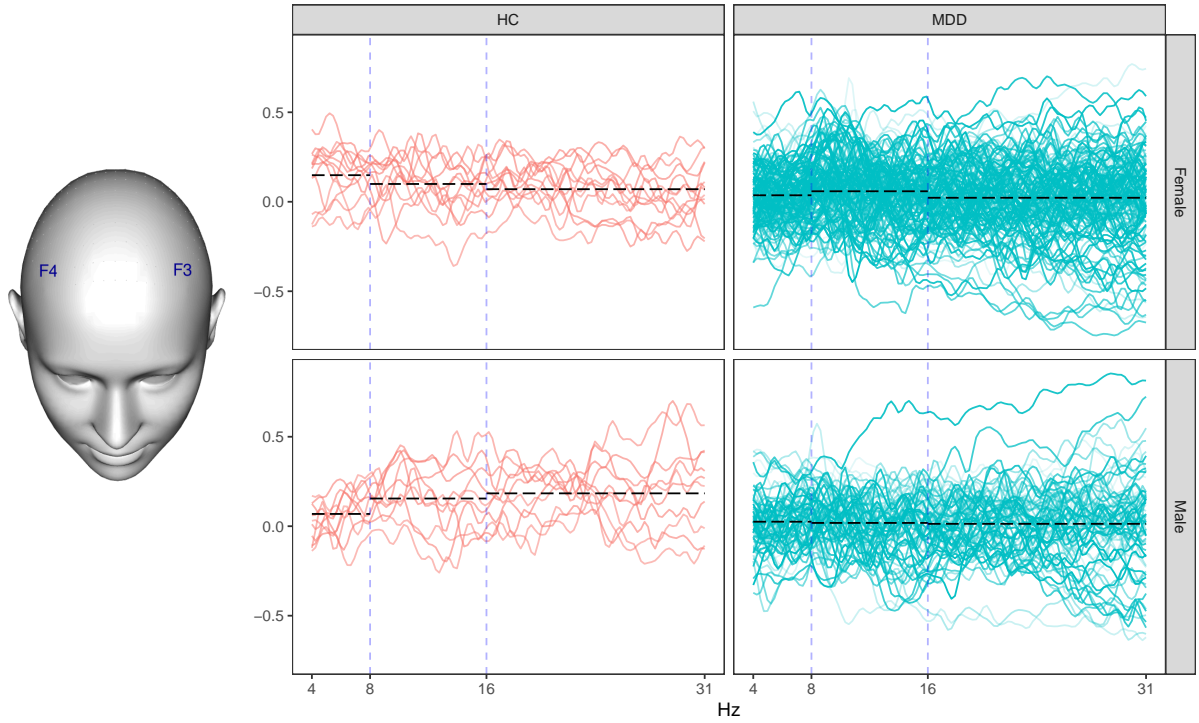


Figure 1: **Left:** Locations of F3 and F4 electrodes. **Right:** Normalized frontal asymmetry curves, $(F4 - F3)/(F4 + F3)$, for each subject with EEG data scored as “Acceptable” or “Good.” HC = healthy control, MDD = major depressive disorder. Blue vertical dashed lines separate the theta (4 - 8 Hz), alpha (8 - 16 Hz), and beta (16 - 31 Hz) frequency bands. Black horizontal dashed lines show mean values within a frequency band.

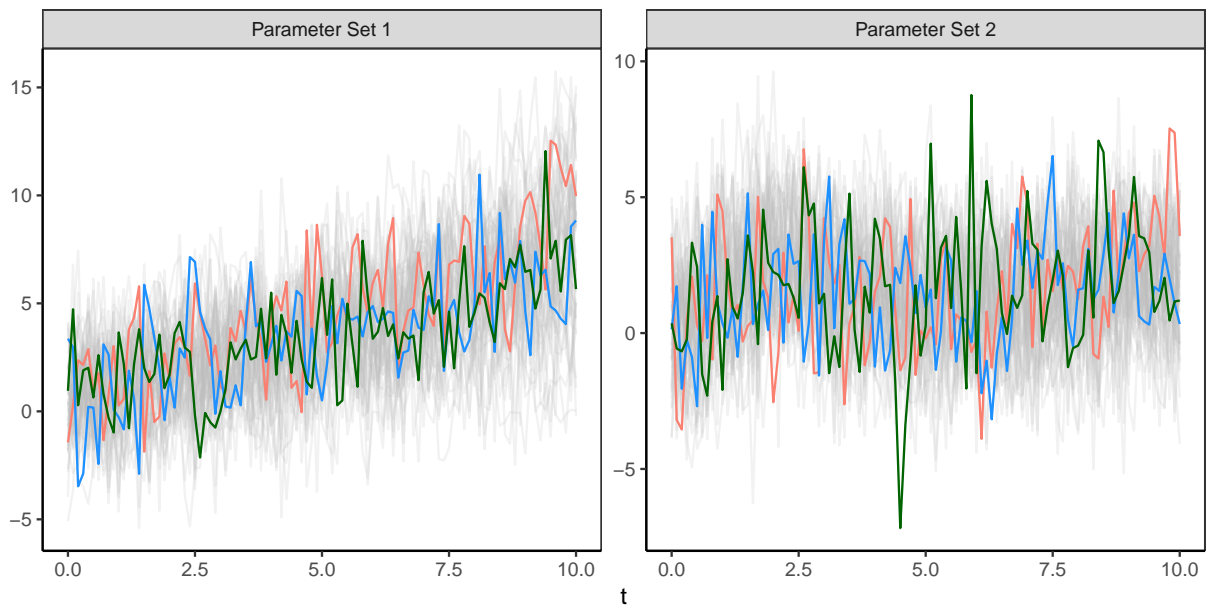


Figure 2: **Left:** 50 simulated responses from Parameter Set 1 with three highlighted observations. **Right:** 50 simulated responses from Parameter Set 2 with three highlighted observations.

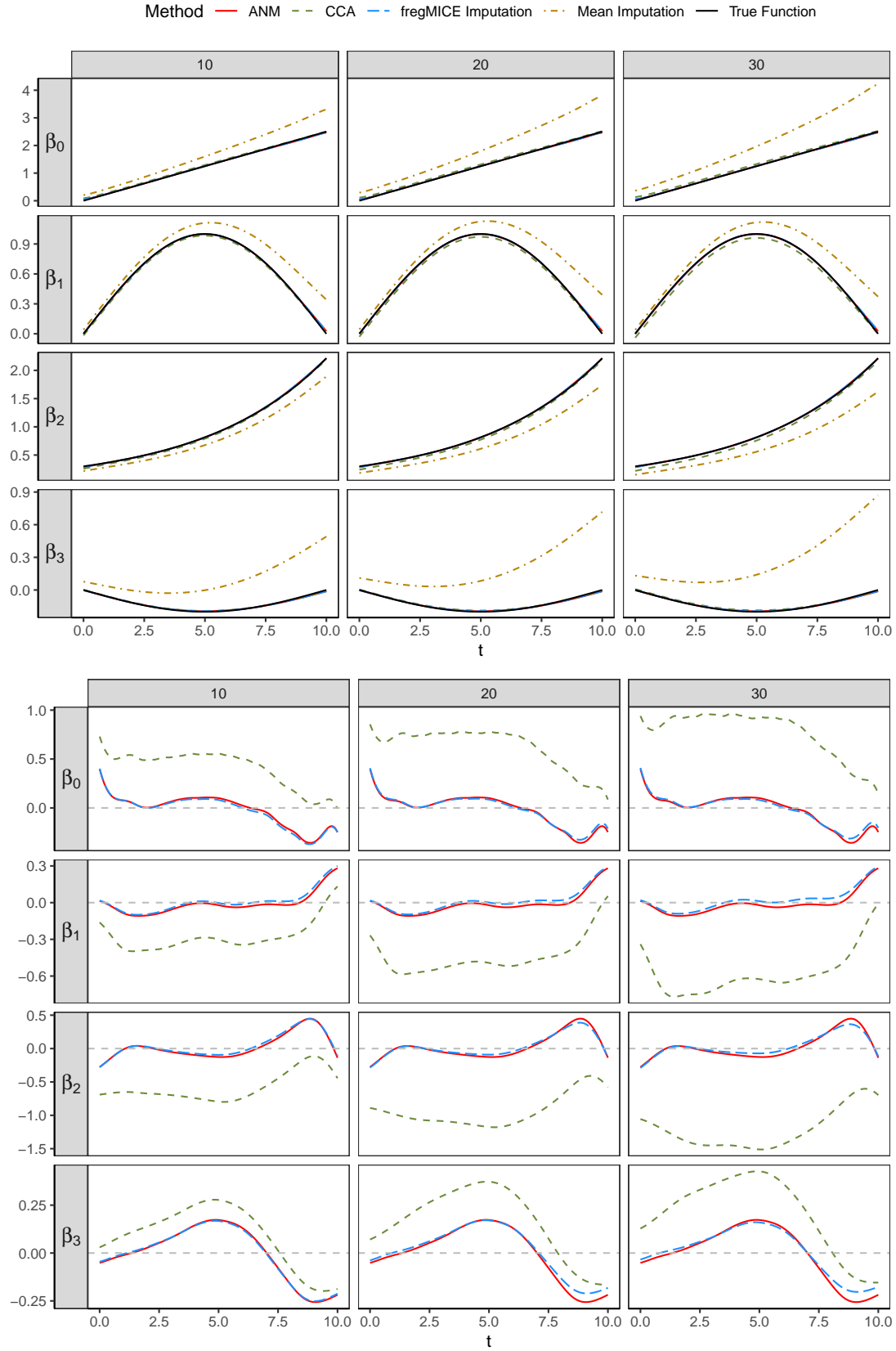


Figure 3: (**Top**) Point-wise mean curves and (**Bottom**) point-wise standardized bias in Setting 1 Scenario (a). Columns (left to right) correspond to 10, 20, and 30% missing data. Rows (top to bottom) correspond to functional parameters $\beta_0, \beta_1, \beta_2$, and β_3 . Point-wise standardized bias curve for mean imputation is removed to better compare estimates from ANM, CCA, and fregMICE.

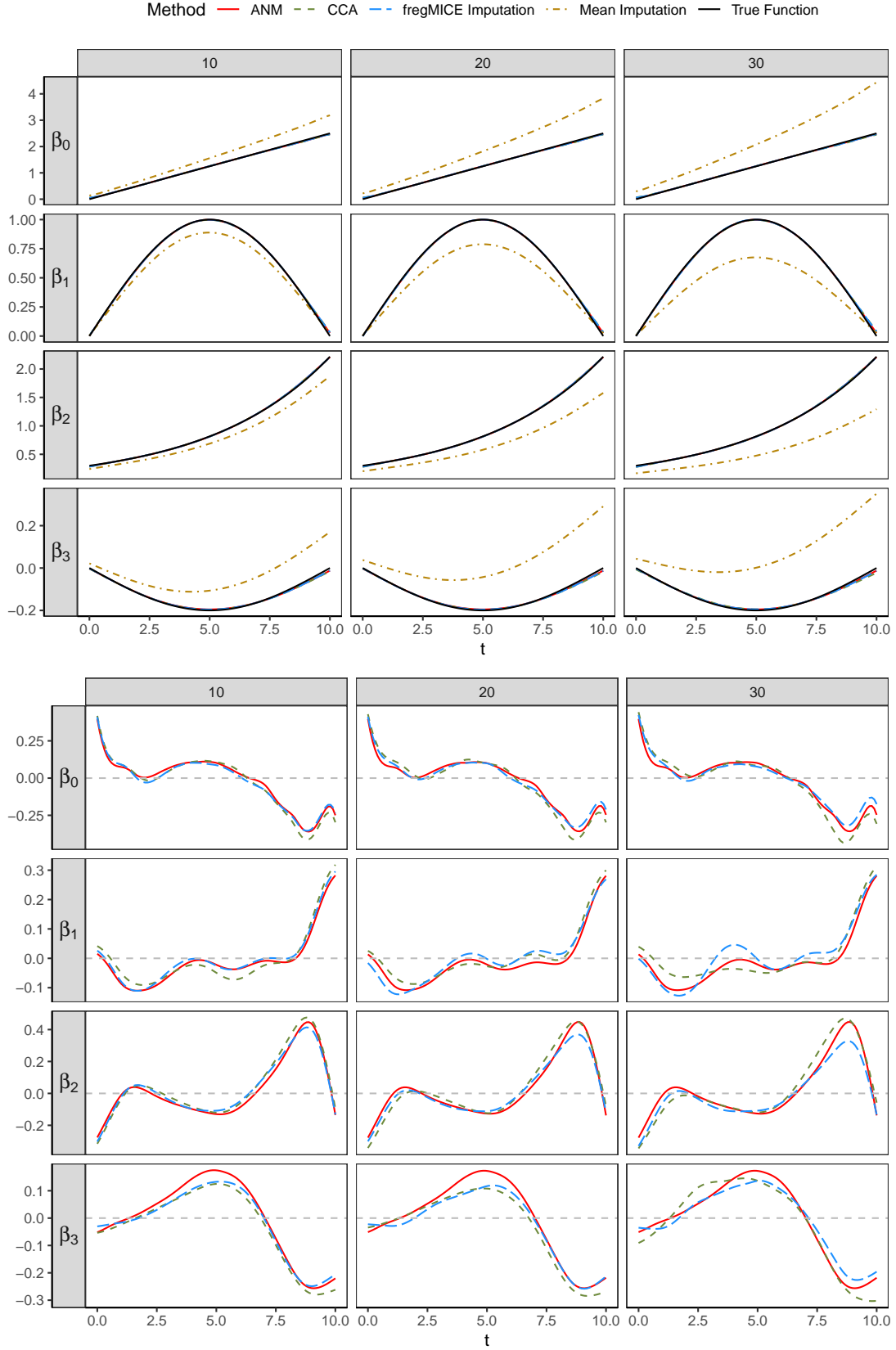


Figure 4: (**Top**) Point-wise mean curves and (**Bottom**) point-wise standardized bias in Setting 1 Scenario (b). Columns (left to right) correspond to 10, 20, and 30% missing data. Rows (top to bottom) correspond to functional parameters $\beta_0, \beta_1, \beta_2$, and β_3 . Point-wise standardized bias curve for mean imputation is removed to better compare estimates from ANM, CCA, and fregMICE.

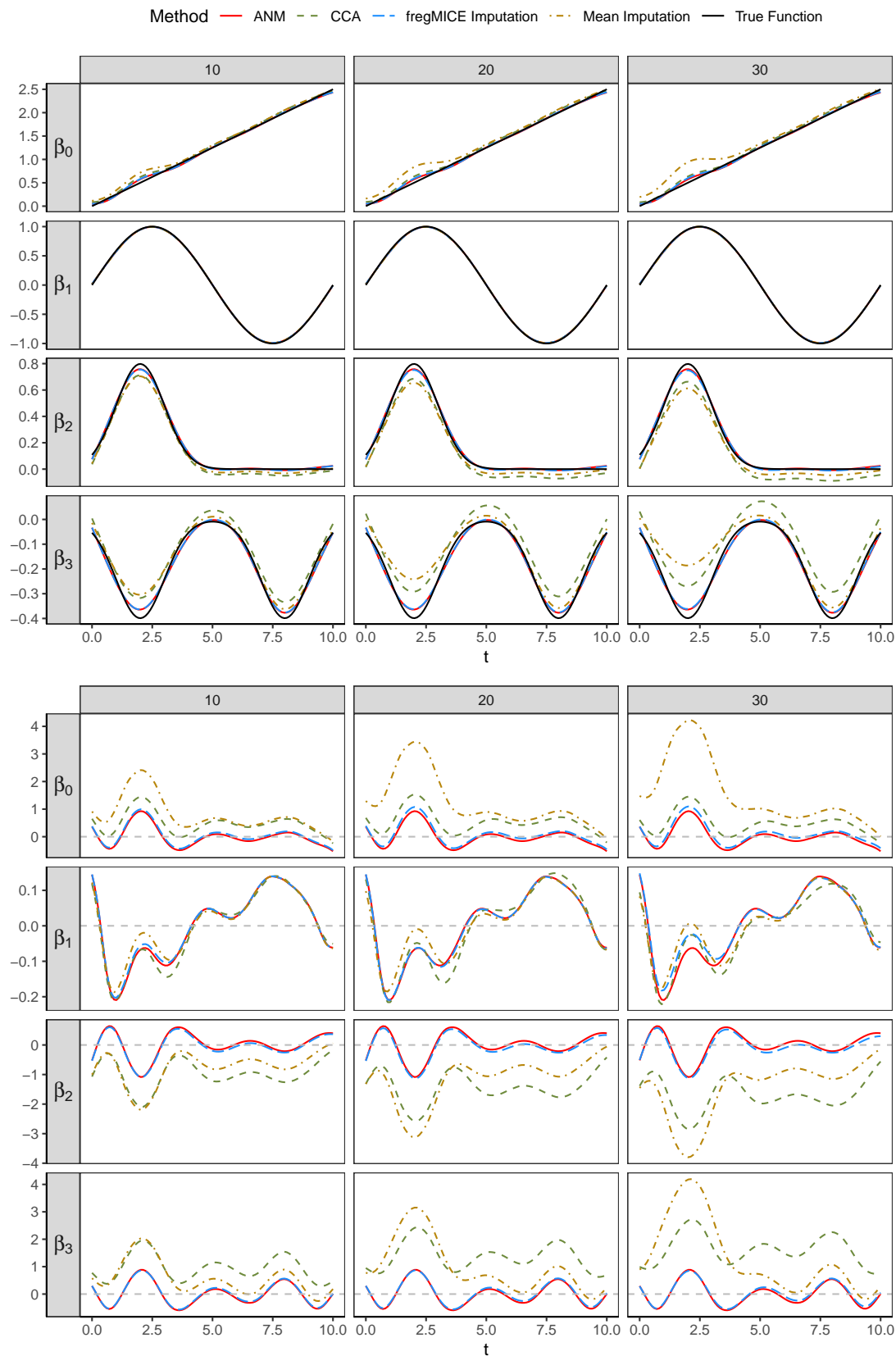


Figure 5: **Top**) Point-wise mean curves and (**Bottom**) point-wise standardized bias in Setting 2 Scenario (a). Columns (left to right) correspond to 10, 20, and 30% missing data. Rows (top to bottom) correspond to functional parameters $\beta_0, \beta_1, \beta_2$, and β_3 .

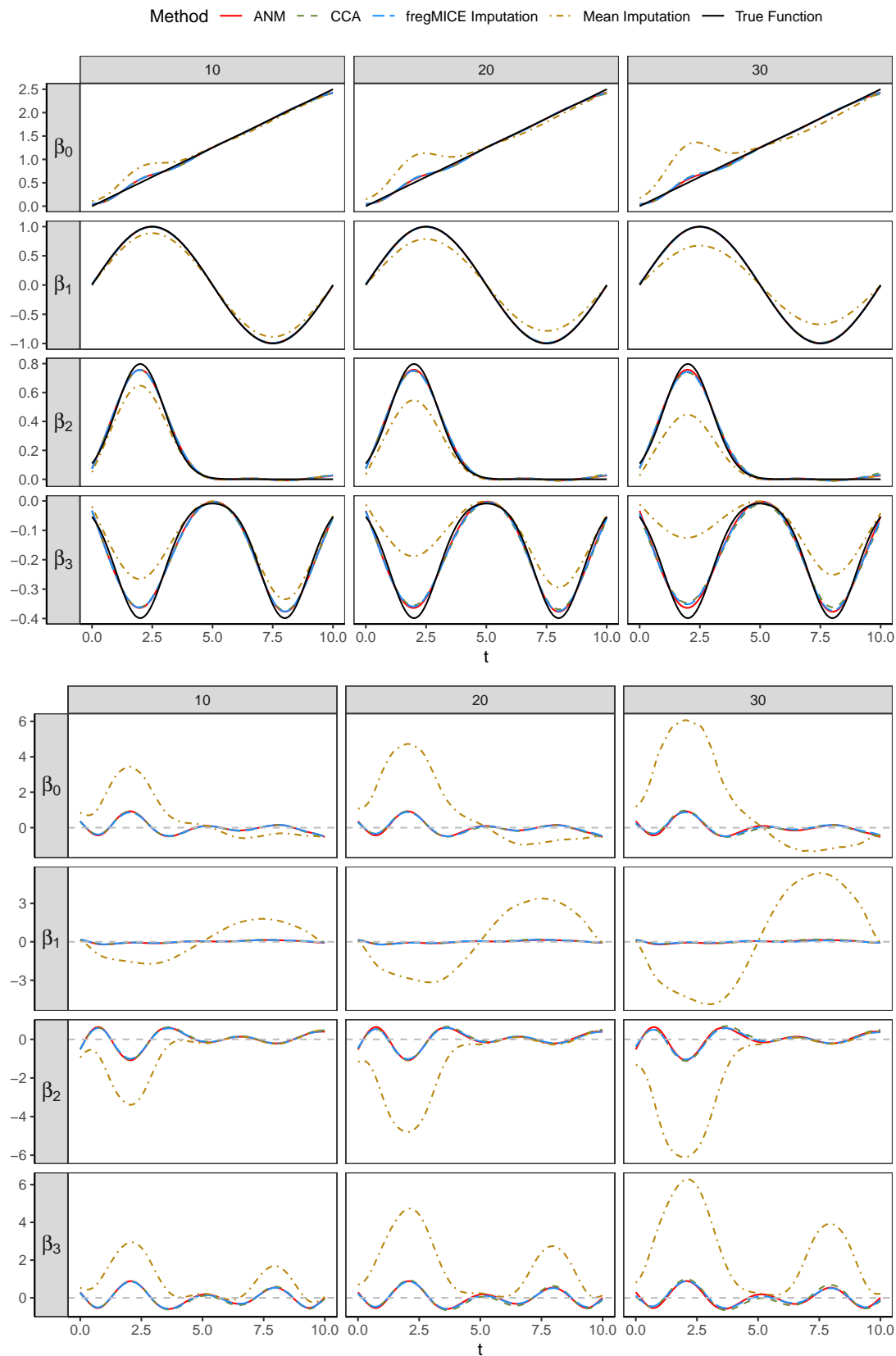


Figure 6: **Top**) Point-wise mean curves and (**Bottom**) point-wise standardized bias in Setting 2 Scenario (b). Columns (left to right) correspond to 10, 20, and 30% missing data. Rows (top to bottom) correspond to functional parameters $\beta_0, \beta_1, \beta_2$, and β_3 .

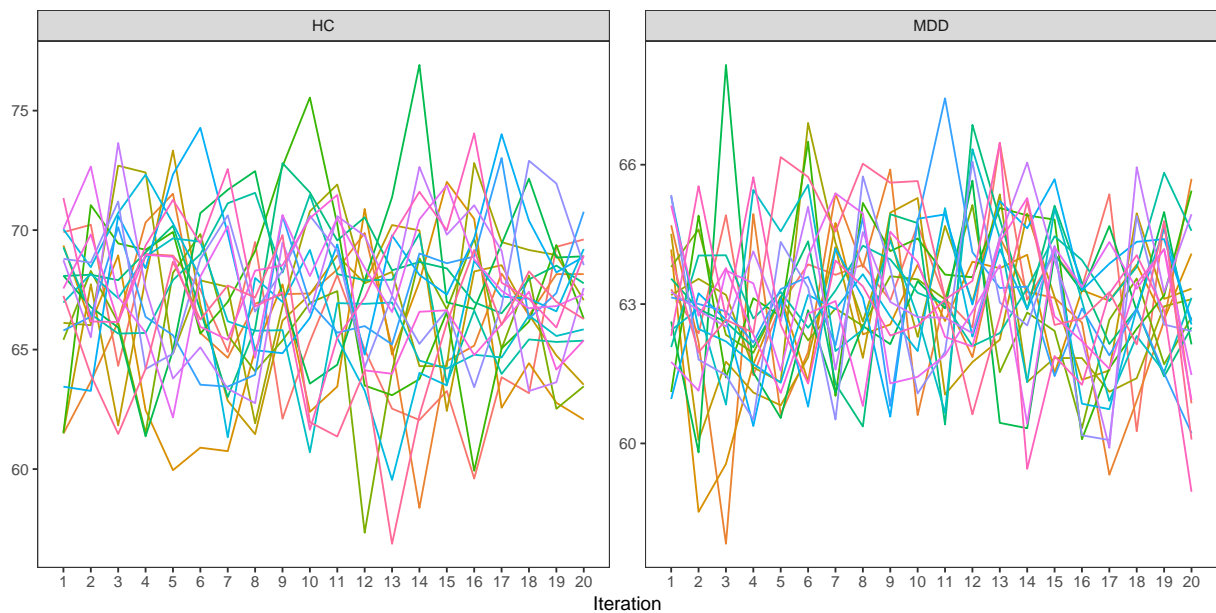


Figure 7: Scalar convergence plots: Mean of the imputed WASIV values for HC and MDD subjects.

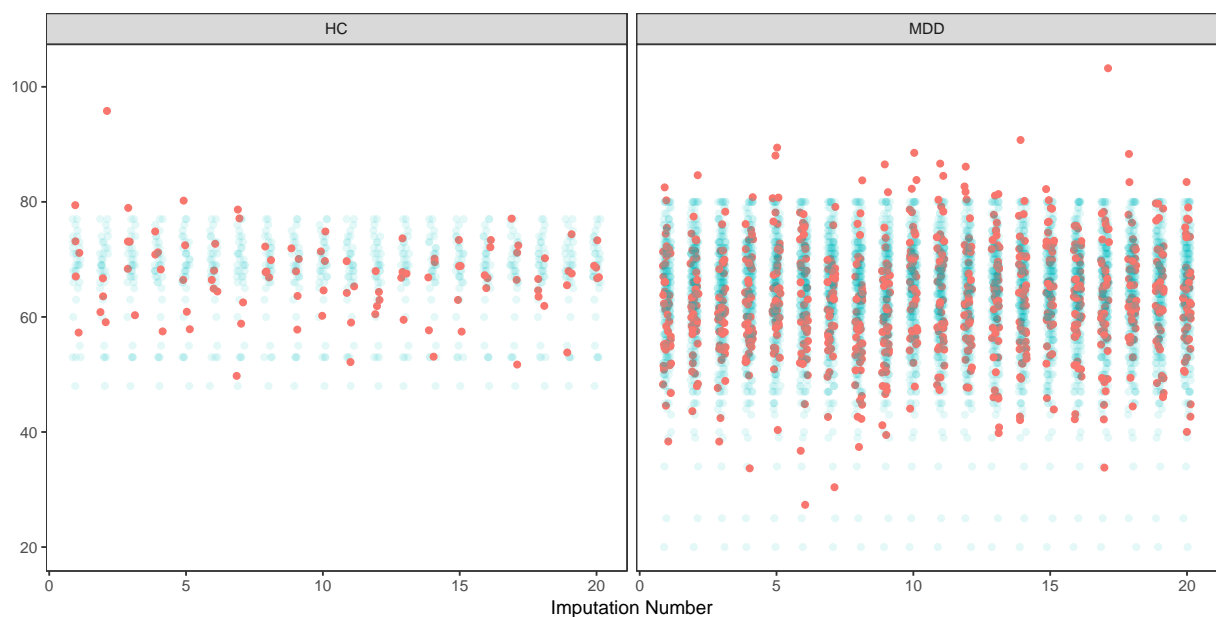


Figure 8: Strip plots of WASIV values. Horizontal axis shows imputation number (m). Vertical axis shows WASIV value. Observed values are blue and imputed values are red.

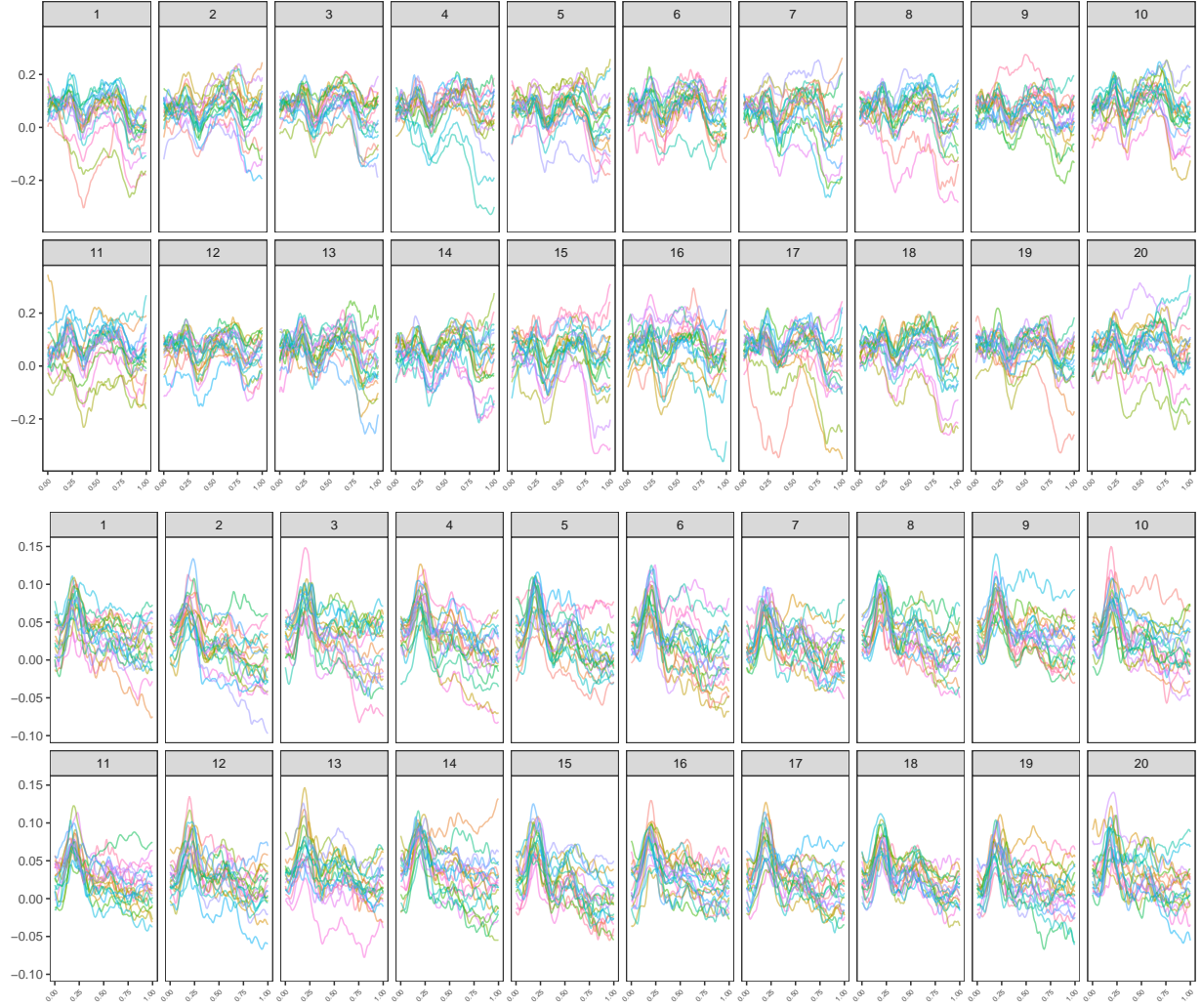


Figure 9: Functional convergence plots. Point-wise mean of the imputed function values for HC (**top 20 panels**) and MDD (**bottom 20 panels**) subjects. Each panel corresponds to an iteration and different colored curves correspond to different imputation streams.

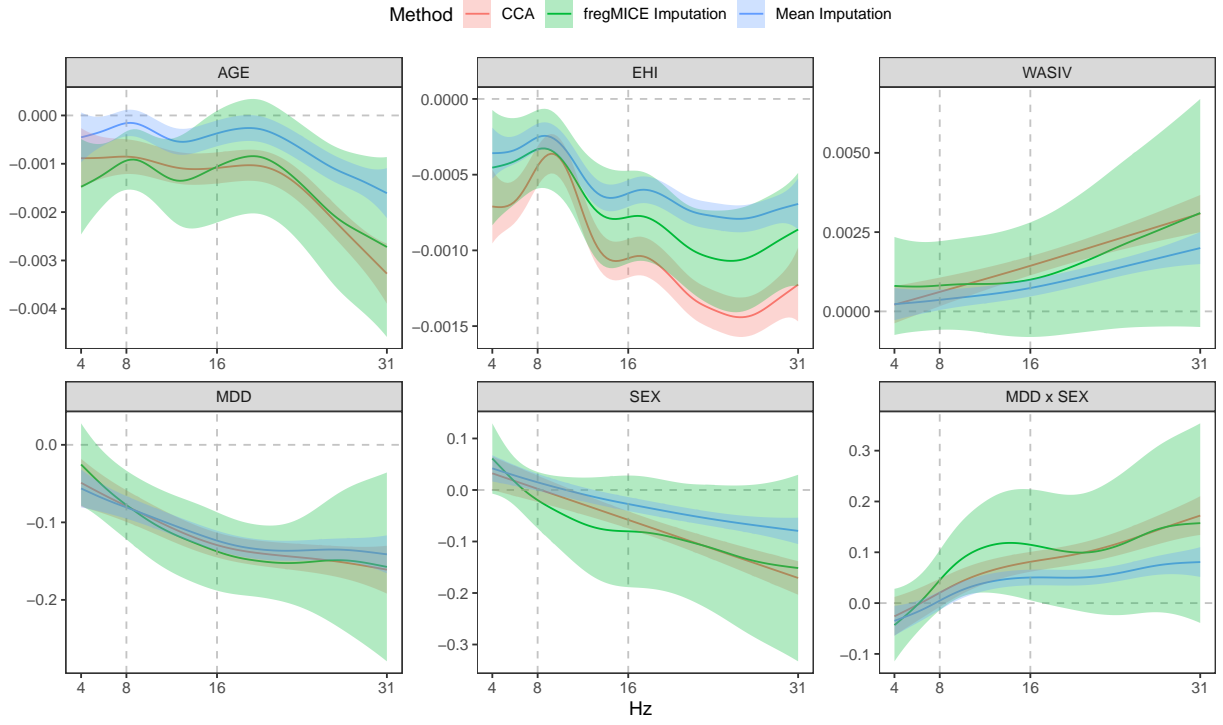


Figure 10: Coefficient function estimates from CCA, fregMICE, and mean imputation.

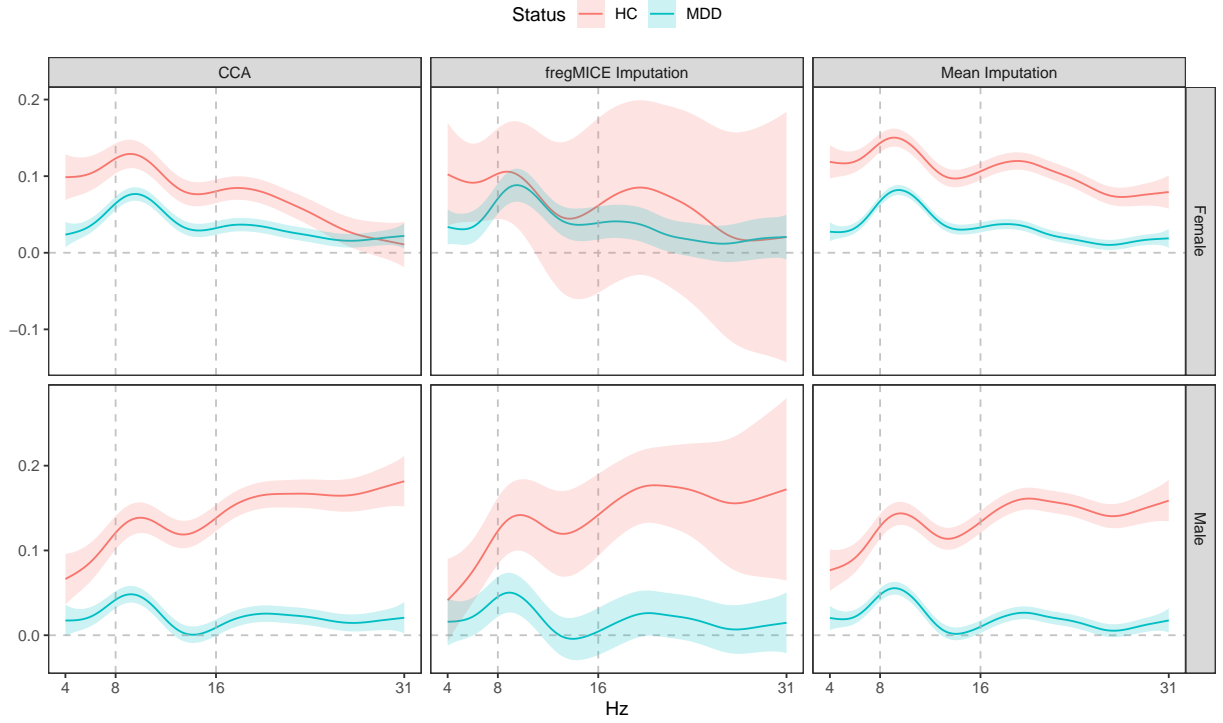


Figure 11: Model-based mean FA curves for subjects with AGE = 37.16, EHI = 71.48, and WASIV = 64.08 based on CCA, fregMICE, and mean imputation.

Table 1: Across-the-function mean point-wise 95% confidence interval coverage (pwCov) and width (pwWidth) for Setting 1 Scenarios (a) and (b).

Scenario (a)		$\hat{\beta}_0(t)$			$\hat{\beta}_1(t)$		
		10%	20%	30%	10%	20%	30%
ANM	pwCov	0.91 (0.10)	0.91 (0.10)	0.91 (0.10)	0.94 (0.09)	0.94 (0.09)	0.94 (0.09)
	pwWidth	0.26 (0.01)	0.26 (0.01)	0.26 (0.01)	0.20 (0.01)	0.20 (0.01)	0.20 (0.01)
Mean	pwCov	0.09 (0.10)	0.02 (0.04)	0.01 (0.02)	0.45 (0.25)	0.42 (0.26)	0.45 (0.27)
	pwWidth	0.28 (0.01)	0.29 (0.01)	0.29 (0.01)	0.21 (0.01)	0.21 (0.01)	0.21 (0.01)
CCA	pwCov	0.87 (0.13)	0.83 (0.16)	0.80 (0.17)	0.92 (0.10)	0.91 (0.12)	0.89 (0.13)
	pwWidth	0.27 (0.01)	0.29 (0.01)	0.30 (0.01)	0.22 (0.01)	0.23 (0.01)	0.25 (0.01)
fregMICE	pwCov	0.90 (0.10)	0.90 (0.11)	0.90 (0.11)	0.94 (0.09)	0.93 (0.10)	0.93 (0.10)
	pwWidth	0.26 (0.01)	0.26 (0.01)	0.27 (0.01)	0.21 (0.01)	0.21 (0.01)	0.22 (0.01)
		$\hat{\beta}_2(t)$			$\hat{\beta}_3(t)$		
		10%	20%	30%	10%	20%	30%
ANM	pwCov	0.92 (0.11)	0.92 (0.11)	0.92 (0.11)	0.91 (0.13)	0.91 (0.13)	0.91 (0.13)
	pwWidth	0.11 (0.00)	0.11 (0.00)	0.11 (0.00)	0.10 (0.01)	0.10 (0.01)	0.10 (0.01)
Mean	pwCov	0.12 (0.12)	0.05 (0.07)	0.03 (0.05)	0.05 (0.06)	0.01 (0.02)	0.01 (0.01)
	pwWidth	0.13 (0.01)	0.15 (0.01)	0.16 (0.01)	0.11 (0.01)	0.11 (0.01)	0.11 (0.01)
CCA	pwCov	0.87 (0.15)	0.80 (0.19)	0.73 (0.21)	0.91 (0.14)	0.90 (0.14)	0.90 (0.14)
	pwWidth	0.13 (0.01)	0.15 (0.01)	0.16 (0.01)	0.11 (0.01)	0.12 (0.01)	0.12 (0.01)
fregMICE	pwCov	0.93 (0.11)	0.93 (0.11)	0.93 (0.12)	0.91 (0.13)	0.91 (0.13)	0.91 (0.13)
	pwWidth	0.12 (0.01)	0.13 (0.01)	0.13 (0.01)	0.11 (0.01)	0.11 (0.01)	0.11 (0.01)
Scenario (b)		$\hat{\beta}_0(t)$			$\hat{\beta}_1(t)$		
		10%	20%	30%	10%	20%	30%
ANM	pwCov	0.91 (0.10)	0.91 (0.10)	0.91 (0.10)	0.94 (0.09)	0.94 (0.09)	0.94 (0.09)
	pwWidth	0.26 (0.01)	0.26 (0.01)	0.26 (0.01)	0.20 (0.01)	0.20 (0.01)	0.20 (0.01)
Mean	pwCov	0.13 (0.11)	0.03 (0.05)	0.01 (0.02)	0.58 (0.25)	0.29 (0.15)	0.18 (0.09)
	pwWidth	0.26 (0.01)	0.25 (0.01)	0.24 (0.01)	0.20 (0.01)	0.19 (0.01)	0.17 (0.01)
CCA	pwCov	0.90 (0.10)	0.90 (0.11)	0.90 (0.11)	0.94 (0.09)	0.94 (0.09)	0.93 (0.10)
	pwWidth	0.28 (0.01)	0.31 (0.01)	0.34 (0.01)	0.22 (0.01)	0.25 (0.01)	0.28 (0.01)
fregMICE	pwCov	0.91 (0.10)	0.91 (0.10)	0.90 (0.11)	0.94 (0.09)	0.94 (0.09)	0.93 (0.10)
	pwWidth	0.28 (0.01)	0.30 (0.02)	0.33 (0.02)	0.22 (0.01)	0.24 (0.02)	0.28 (0.03)
		$\hat{\beta}_2(t)$			$\hat{\beta}_3(t)$		
		10%	20%	30%	10%	20%	30%
ANM	pwCov	0.92 (0.11)	0.92 (0.11)	0.92 (0.11)	0.91 (0.13)	0.91 (0.13)	0.91 (0.13)
	pwWidth	0.11 (0.00)	0.11 (0.00)	0.11 (0.00)	0.10 (0.01)	0.10 (0.01)	0.10 (0.01)
Mean	pwCov	0.15 (0.13)	0.03 (0.04)	0.01 (0.02)	0.24 (0.20)	0.09 (0.07)	0.05 (0.04)
	pwWidth	0.11 (0.00)	0.11 (0.01)	0.11 (0.01)	0.10 (0.01)	0.10 (0.01)	0.09 (0.01)
CCA	pwCov	0.93 (0.10)	0.92 (0.11)	0.92 (0.11)	0.91 (0.13)	0.91 (0.14)	0.90 (0.15)
	pwWidth	0.12 (0.01)	0.14 (0.01)	0.15 (0.01)	0.11 (0.01)	0.13 (0.01)	0.14 (0.01)
fregMICE	pwCov	0.93 (0.11)	0.93 (0.10)	0.93 (0.11)	0.92 (0.12)	0.92 (0.12)	0.91 (0.13)
	pwWidth	0.12 (0.01)	0.14 (0.01)	0.15 (0.02)	0.12 (0.01)	0.13 (0.02)	0.15 (0.02)

Table 2: Across-the-function mean point-wise 95% confidence interval coverage (pwCov) and width (pwWidth) for Setting 2 Scenarios (a) and (b).

Scenario (a)		$\hat{\beta}_0(t)$			$\hat{\beta}_1(t)$		
		10%	20%	30%	10%	20%	30%
ANM	pwCov	0.91 (0.08)	0.91 (0.08)	0.91 (0.08)	0.94 (0.08)	0.94 (0.08)	0.94 (0.08)
	pwWidth	0.30 (0.01)	0.30 (0.01)	0.30 (0.01)	0.25 (0.01)	0.25 (0.01)	0.25 (0.01)
Mean	pwCov	0.79 (0.12)	0.67 (0.12)	0.60 (0.12)	0.93 (0.08)	0.93 (0.08)	0.92 (0.09)
	pwWidth	0.31 (0.01)	0.31 (0.01)	0.32 (0.01)	0.25 (0.01)	0.25 (0.01)	0.25 (0.01)
CCA	pwCov	0.87 (0.10)	0.87 (0.10)	0.88 (0.10)	0.94 (0.08)	0.94 (0.07)	0.94 (0.08)
	pwWidth	0.32 (0.01)	0.33 (0.01)	0.34 (0.01)	0.26 (0.01)	0.27 (0.01)	0.29 (0.01)
fregMICE	pwCov	0.91 (0.08)	0.91 (0.09)	0.90 (0.09)	0.94 (0.08)	0.94 (0.08)	0.94 (0.08)
	pwWidth	0.31 (0.01)	0.32 (0.01)	0.33 (0.01)	0.25 (0.01)	0.25 (0.01)	0.25 (0.01)
		$\hat{\beta}_2(t)$			$\hat{\beta}_3(t)$		
		10%	20%	30%	10%	20%	30%
ANM	pwCov	0.91 (0.08)	0.91 (0.08)	0.91 (0.08)	0.90 (0.09)	0.90 (0.09)	0.90 (0.09)
	pwWidth	0.14 (0.00)	0.14 (0.00)	0.14 (0.00)	0.15 (0.01)	0.15 (0.01)	0.15 (0.01)
Mean	pwCov	0.82 (0.12)	0.71 (0.13)	0.64 (0.13)	0.81 (0.12)	0.70 (0.11)	0.63 (0.10)
	pwWidth	0.15 (0.00)	0.16 (0.01)	0.16 (0.01)	0.14 (0.01)	0.14 (0.01)	0.14 (0.01)
CCA	pwCov	0.79 (0.13)	0.67 (0.15)	0.57 (0.14)	0.79 (0.13)	0.67 (0.15)	0.58 (0.15)
	pwWidth	0.16 (0.01)	0.17 (0.01)	0.18 (0.01)	0.16 (0.01)	0.17 (0.01)	0.18 (0.01)
fregMICE	pwCov	0.91 (0.09)	0.91 (0.09)	0.92 (0.09)	0.91 (0.09)	0.91 (0.08)	0.91 (0.09)
	pwWidth	0.15 (0.01)	0.16 (0.01)	0.17 (0.01)	0.15 (0.01)	0.15 (0.01)	0.16 (0.01)
Scenario (b)		$\hat{\beta}_0(t)$			$\hat{\beta}_1(t)$		
		10%	20%	30%	10%	20%	30%
ANM	pwCov	0.91 (0.08)	0.91 (0.08)	0.91 (0.08)	0.94 (0.08)	0.94 (0.08)	0.94 (0.08)
	pwWidth	0.30 (0.01)	0.30 (0.01)	0.30 (0.01)	0.25 (0.01)	0.25 (0.01)	0.25 (0.01)
Mean	pwCov	0.70 (0.12)	0.57 (0.12)	0.46 (0.13)	0.69 (0.17)	0.37 (0.13)	0.21 (0.06)
	pwWidth	0.29 (0.01)	0.29 (0.01)	0.28 (0.01)	0.23 (0.01)	0.22 (0.01)	0.20 (0.01)
CCA	pwCov	0.91 (0.09)	0.91 (0.09)	0.90 (0.09)	0.94 (0.08)	0.94 (0.08)	0.93 (0.08)
	pwWidth	0.33 (0.01)	0.36 (0.01)	0.40 (0.02)	0.27 (0.01)	0.30 (0.01)	0.34 (0.01)
fregMICE	pwCov	0.92 (0.08)	0.91 (0.08)	0.91 (0.09)	0.94 (0.08)	0.94 (0.08)	0.93 (0.08)
	pwWidth	0.33 (0.01)	0.36 (0.02)	0.40 (0.03)	0.27 (0.01)	0.29 (0.01)	0.32 (0.02)
		$\hat{\beta}_2(t)$			$\hat{\beta}_3(t)$		
		10%	20%	30%	10%	20%	30%
ANM	pwCov	0.91 (0.08)	0.91 (0.08)	0.91 (0.08)	0.90 (0.09)	0.90 (0.09)	0.90 (0.09)
	pwWidth	0.14 (0.00)	0.14 (0.00)	0.14 (0.00)	0.15 (0.01)	0.15 (0.01)	0.15 (0.01)
Mean	pwCov	0.76 (0.09)	0.66 (0.09)	0.61 (0.09)	0.72 (0.11)	0.54 (0.10)	0.41 (0.08)
	pwWidth	0.14 (0.00)	0.14 (0.01)	0.13 (0.01)	0.13 (0.01)	0.12 (0.01)	0.11 (0.01)
CCA	pwCov	0.92 (0.08)	0.91 (0.08)	0.91 (0.09)	0.91 (0.09)	0.90 (0.09)	0.90 (0.10)
	pwWidth	0.16 (0.01)	0.17 (0.01)	0.19 (0.01)	0.16 (0.01)	0.18 (0.01)	0.20 (0.01)
fregMICE	pwCov	0.92 (0.08)	0.92 (0.08)	0.91 (0.08)	0.91 (0.09)	0.91 (0.09)	0.91 (0.09)
	pwWidth	0.16 (0.01)	0.17 (0.01)	0.20 (0.01)	0.16 (0.01)	0.17 (0.01)	0.19 (0.02)

Table 3: Summary statistics for variables in the analysis model.

Variable	n Available	Mean (SD) or n (%)
AGE	335	37.16 (13.46)
EH1	335	71.48 (48.54)
WASIV	286	64.08 (9.41)
MDD (MDD)	335	295 (88.1)
SEX (Female)	335	218 (65.1)
FA	324	
Good		143 (42.7)
Acceptable		93 (27.8)
Marginal		58 (17.3)
Unacceptable		30 (9.0)
Missing		11 (3.3)